Appendix A

A1 Microscopic investigations

A1.1 Introduction

The objective of the investigation was to explain the non-linear geomechanical behaviour of the rock samples from the Impala 10-shaft instrumentation site (Impala). From the literature review it was apparent that the following should be studied:

- The bulk rock composition, textural relations and mineral associations;
- the nature and amount of cementing medium;
- the fabric; and
- the stress history of the rock for early stage compaction to late stage cooling.

Descriptions of these concepts are provided in the literature review.

Standard X-ray Fluorescence (XRF) techniques were conducted to study the chemical composition of rock specimens from Impala, Union Section Spud-shaft (Union) and Amandelbult 1-shaft (Amandelbult) to determine if the there was a chemical difference between the linear and nonlinear elastic samples. The micro fracturing was investigated using slides prepared from most of the hangingwall rock types in both the vertical and horizontal directions from Impala and Union. The results were compared to rock specimens with a more linear stress-strain relationship from Amandelbult. Optical microscopic observations revealed the presence of microfractures but it could not be determined whether the fractures are open or closed. In this regard, a Scanning Electron Microscope (SEM) was used to conduct observations on polished sections of leuconorite/anorthosite samples from Amandelbult and Impala.

A1.2 Literature review

A1.2.1 Bulk rock composition, textual relations and mineral associations

Wilson et al. (2005) calculated normative compositions from the major element analyses. They found unexpected correlations between the uniaxial compressive strength (UCS) of the rocks and zircon (Zr, in parts per million (ppm)) and normative quartz in volume percent (vol %) in the whole rock. The Zr contents vary from about 1 to 10.5 ppm. The normative quartz contents vary from less than 0.1 to about 1.8 vol%.

Image analysis was used by Wilson et al. (2005) to study the textures and mineral associations of the core samples. They concluded that rocks with widely differing textures have very similar mineralogical compositions, so that there is no definitive textural control on rock strength. In addition, many of the samples analysed indicate a major and minor structural grain at higher angles to the vertical than the plane of layering. They postulate that these developed as a result of compaction shearing. Further research is recommended.

Plagioclase has one perfect cleavage plane {001} and another good one {010} (Hurlbut and Klein, 1977). If a plagioclase crystal is broken, it will mostly break along these cleavage planes. Orthopyroxene has one good cleavage plane {210}, with a good parting on {100} (Hurlbut and Klein, 1977). Breakage of an orthopyroxene grain will most likely occur along these planes.

Minor minerals are considered to form a small percentage of the total rock volume. An example would be Biotite, with its distinctive reddish-brown colour and prominent pleochroism. This colour is characteristic of titanium-rich biotite (Heinrich, 1965). It commonly encloses an opaque black mineral, either magnetite or ilmenite.

A1.2.2 The nature and amount of cementing medium

A small amount of quartz was observed by Wilson et al. (2005) in some of the samples studied. The quartz occurs along the grain boundaries, and appears to have an effect on the way fractures propagate throughout the rock. In addition, the Zr content of the rock is taken by Wilson et al. (2005) as a proxy for the very late stage minerals that crystallized from the magma, and that might form cement between the earlier formed grains. Wilson and co-workers did not report the

observation of zircon grains in their study. This is not surprising given the less than 12 ppm levels of Zr in the whole rock analyses. A larger database of geochemical analyses and UCS tests is needed before definitive conclusions can be drawn.

A1.2.3 Fabric

The Bushveld Complex is layered from large scale down to millimetre thickness layering. This layering is the result of different mineral compositions within the layers. Contacts between layers may be abrupt or gradational. Within the layer, the mineral crystal grains that constitute it may or may not show a preferred orientation with respect to the crystallographic axes of the mineral. Tabular and lath-shaped mineral grains may settle with their long axes parallel or sub-parallel to the layering, giving rise to a fabric. Such a fabric would result in anisotropic behaviour with respect to rock properties such as magnetism and seismic velocity.

Wilson et al. (2005) examined two rocks using image analysis to determine whether grain-fabric and grain-size have an influence on the UCS of the rock. They concluded that the norite sample with smaller grains that are more randomly orientated was stronger than a coarser grained norite that displayed some alignment of mineral grains. Further research is suggested.

A1.2.4 Stress history of the rock for early stage compaction to late stage cooling

The stress history of the Bushveld rocks may have an influence on their mechanical behaviour (Wilson et al, 2005). This stress history includes the settling of the minerals, the compaction of the minerals into layers and the subsequent cooling (and contraction) of these layers.

Fluid pressure in the pores of a rock has a significant effect on its strength (Wilson et al, 2005). The studied rocks were characterized as massive with very low porosity levels. However, the possibility that early trapped fluids could have produced hydrous interstitial minerals that might have affected the UCS readings was considered. It is assumed that in massive unaltered rock (fresh rock) there is minimal interconnectivity of pores, and hence fluids in non-porous igneous rocks will only affect short range propagation of fractures. This is in contrast with certain

types of sedimentary rocks such as sandstone and limestone which may have well-developed porosities.

In addition to the above factors, microfracturing in the rock has been recognized as playing an important role in rock mass behaviour (Kranz, 1983; Johnson and Rasolofosaon, 1996; Lyakhovsky et al., 1997 and Bucur and Rasolofosaon, 1998).

Recent studies indicate that the nonlinear elastic behaviour of brittle rocks, especially at low stress levels, may be attributed to pre-existing open microcracks in the rock (Li et al, 1998; Ryder and Jager, 2002; Lavrov, 2005). These open microcracks may be randomly orientated or show a preferred orientation (due to crystal grain orientation), and will close when the rock is subjected to compression. Li et al. (1998) studied the stress-strain behaviour of rocks related to fracture under compression, and concluded that the nonlinear "toe" of the axial stress-strain curve is due to the closure of open cracks. The shape of the toe is dependent on the aspect ratio of the pre-existing crack, defined as the ratio of the crack opening to length.

A1.3 Results of the optical microscopic and XRF investigations

A1.3.1 Bulk rock composition, textual relations and mineral associations

The Impala rocks are composed mainly of plagioclase feldspar, orthopyroxene and minor quantities of clinopyroxene. In the leuconorites and norites, the plagioclase forms a cumulate framework with interstitial orthopyroxene and minor clinopyroxene. In the melanorites and pyroxenites, orthopyroxene forms a cumulate framework with minor clinopyroxene and interstitial plagioclase. The plagioclase crystals are from fine to medium grained in size, and display the range of typical plagioclase twinning, including Carlsbad, albite and periclinal sets. The rock specimen from Union is a melanorite, with orthopyroxene and minor clinopyroxene forming a cumulate framework with interstitial plagioclase. The rock types from Amandelbult are comprised mainly of plagioclase and orthopyroxene, with minor clinopyroxene and biotite. The detailed XRF investigation is included in Appendix A2.

Although the sample set is small, the major geochemical compositions for equivalent rock types from Impala and Amandelbult are the same. The Union sample has no exact major element geochemical equivalent with either the Impala or the Amandelbult suites. This is interpreted to indicate an intermediate mineralogical composition that will fit in with the gradational changes in the rock compositions from anorthosites to pyroxenites. Correlations were found between percentages of some minerals and UCS. However, these relationships could only explain the variation in strength but not the non-linear stress-strain behaviour. On a gross scale, the plagioclase-rich rocks have higher UCS values than the more orthopyroxene-rich rocks. In general, the UCS tests show that the Amandelbult rocks have the lowest Poisson's Ratios. The reason for this is not evident from the major element comparisons. The trace element contents of the rocks from the three mines also do not explain the observed non-linear, stress-strain behaviour.

A1.3.2 The nature and amount of cementing medium

Substantial differences in the cementing medium could not be determined between the three sites. Biotite was observed as small grains along pyroxene-plagioclase grain boundaries. Since there was no substantial difference in the cementing medium at the three sites, this does not appear to offer an explanation to the nonlinear stress-strain behaviour of the rocks at the Impala site.

A1.3.3 Fabric

A weak alignment of subvertical plagioclase crystals were observed perpendicular to layering in one slide from Impala (Figure A1 1). This alignment probably indicates syn-magmatic "imbrication" of plagioclase during magma crystallisation. Samples of this rock type were tested in directions perpendicular and parallel to the stratification but no difference in the behaviour was observed. It is thus concluded that the alignment shown in Figure A1 1 had no effect or only a weak influence on the mechanical behaviour of the rock. The fabric does not appear to explain the nonlinear stress-strain behaviour of the Impala rocks.

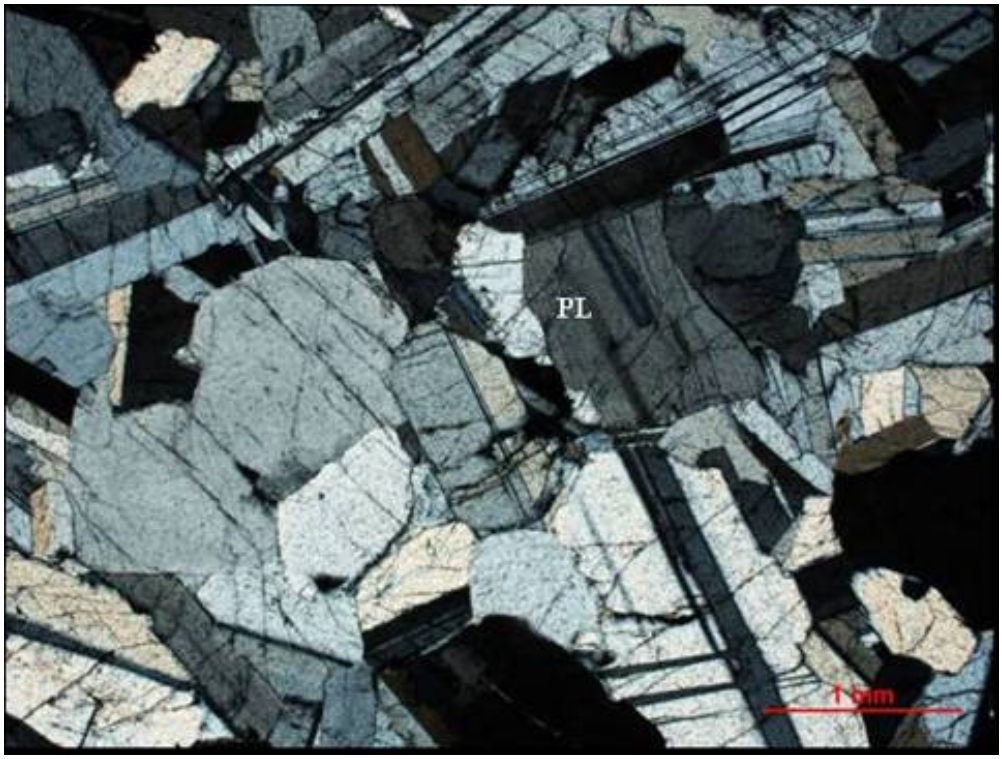

Figure A1 1 Localised areas of weak alignment of plagioclase (PL) crystals perpendicular to layering from Impala 10-shaft

A1.3.4 Stress history of the rock for early stage compaction to late stage cooling

Optical microscopic observations revealed the common occurrence of microfractures within the rocks from all three sites. The task was challenging because of the different appearance of the fractures in the plagioclase and the orthopyroxene under microscopic conditions. Orthopyroxene has a high relative relief to that of plagioclase and as a result fractures in orthopyroxene are more prominent than those present in plagioclase. This can result in subjectivity regarding the volume of fractures and their nature (open or closed). Fractures were observed in all directions and could therefore be considered to be randomly distributed. Dominant directions were, however, observed in the pyroxenes but not in the plagioclase at Impala. In addition, there were no obvious differences in the micro-fracturing of samples that were compressed to failure in a test laboratory and those that had not been geomechanically tested. One representative slide from each of the three sites is provided in Figure A1 2 to Figure A1 4. The full investigation is shown in Appendix A3.

Figure A1 2 shows some fracture patterns in a pyroxenite from Impala. The fractures in the orthopyroxene crystals (in green) show a dominant trend that extends across the whole field of view from top left to bottom right. This dominant trend is not strongly defined but still visible in the interstitial plagioclase (in orange).

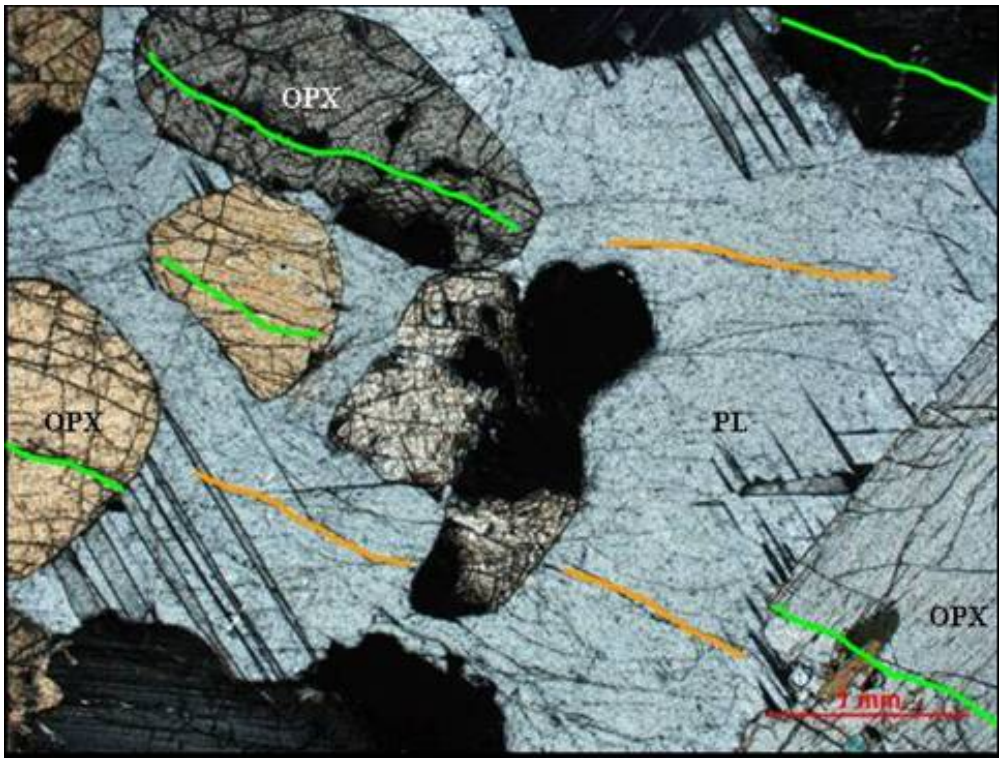

Figure A1 2 Fracture patterns observed under cross polarised light. The fractures in the orthopyroxene (OPX) and plagioclase (PL) crystals are in green and orange respectively. The pyroxenite sample is from Impala

The specimen from Union was highly fractured, with the microfractures cutting through both pyroxene and plagioclase (Figure A1 3).

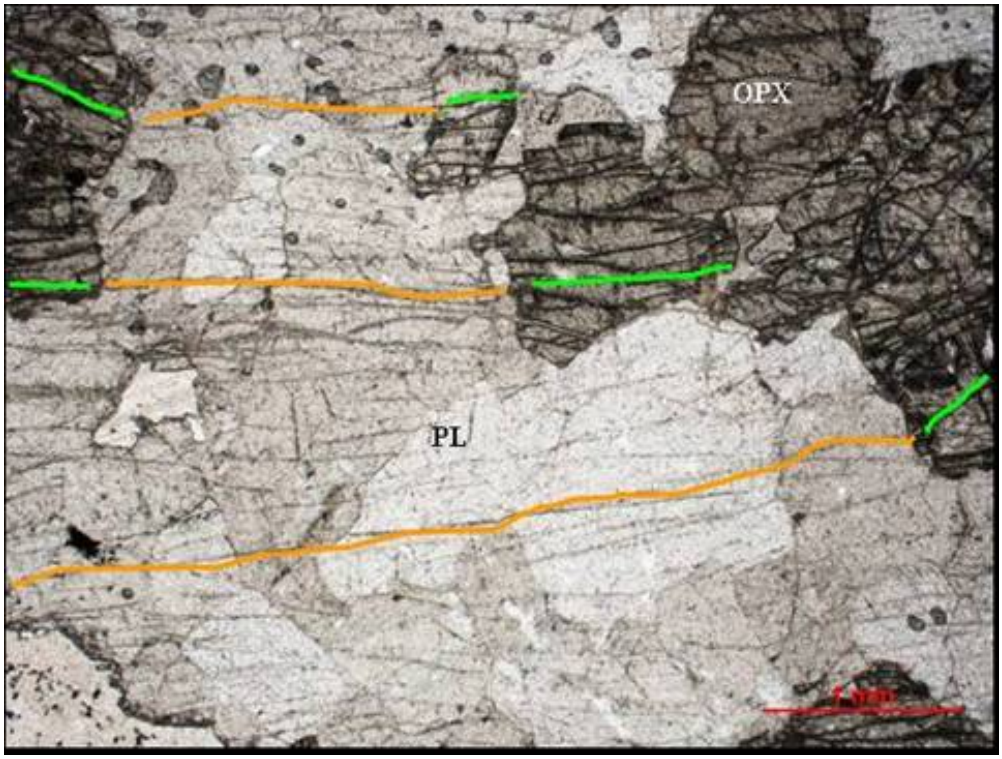

Figure A1 3 The sample from Union shows sinuous yet continuous fractures that cut across both the orthopyroxene and the plagioclase crystals

The samples from Amandelbult show a difference in the amount of fracturing between the rock types. In the suite of samples supplied, anorthosite is the least fractured, with the two melanorites being the most fractured. In the latter, the orthopyroxene crystals carry the most fracturing. Figure A1 4 shows the preferred orientation of the fractures in the orthopyroxene of an anorthosite sample, which does not extend across the surrounding plagioclase. It is suggested that these fractures relate to the 90° cleavage planes of the orthopyroxene. The fracturing in the plagioclase of this sample does not show a preferred orientation and do not appear to be laterally extensive.

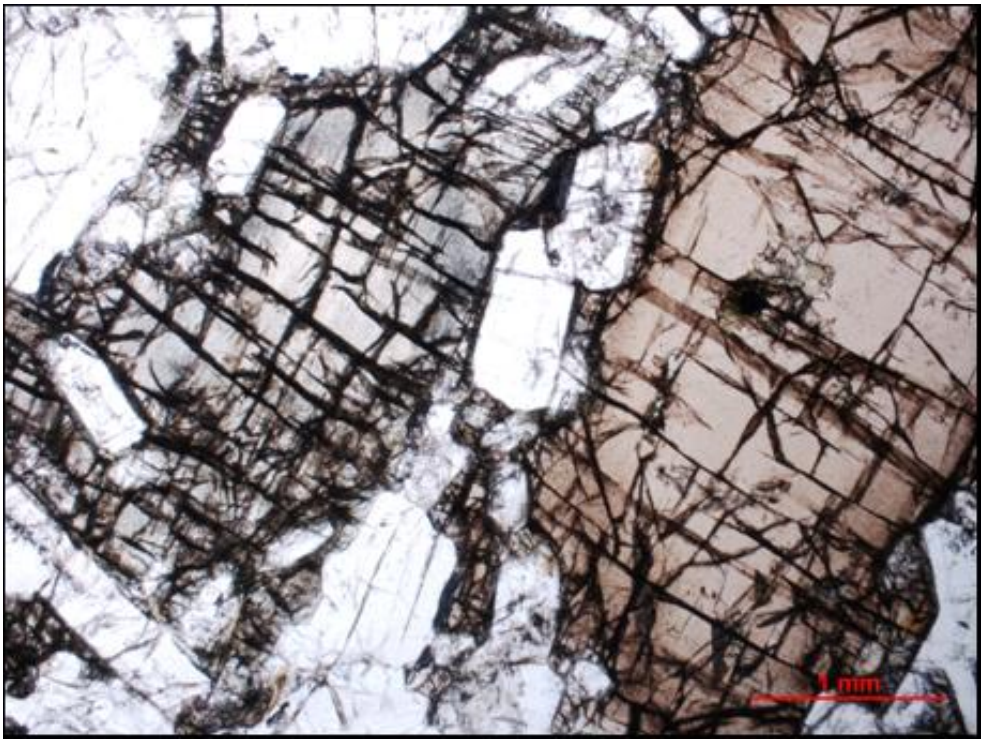

Figure A1 4 Fracturing in orthopyroxene of an anorthosite sample

Since there were no obvious differences in the mineralogy or fracturing between the three sites, further investigations were needed. A scanning electron microscope (SEM) was used to determine whether the non linear behaviour of the Impala rocks could be attributed to open fractures.

A1.4 Results of the SEM analysis

Two samples were used in the investigation to compare the nonlinear stress-strain behaviour rocks from Impala to the more linear rocks from Amandelbult. The results of the investigation showed that the microfractures were more numerous and better developed in the orthopyroxene than in the plagioclase crystals in both samples. It was difficult to observe conclusively whether the microfractures were open or closed in the sample from Amandelbult site, even under very high magnification. However, there was more definite evidence of open fractures in the Impala sample, both in the orthopyroxene and plagioclase crystals. Some of the micro fractures from both sites were filled with material of similar compositions to the host mineral and some sulphides were also clearly

visible in the microfractures. These fractures were obviously *in situ* prior to mining. The full investigation is shown in Appendix A4.

Figure A1 5 shows two photographs of the microfracturing in the sample from the Amandelbult site. The images clearly show that the number and development of the fractures in the orthopyroxene (A) and plagioclase (B) crystals were different. Significantly fewer fractures were observed in the plagioclase. The microfractures appear to be closed.

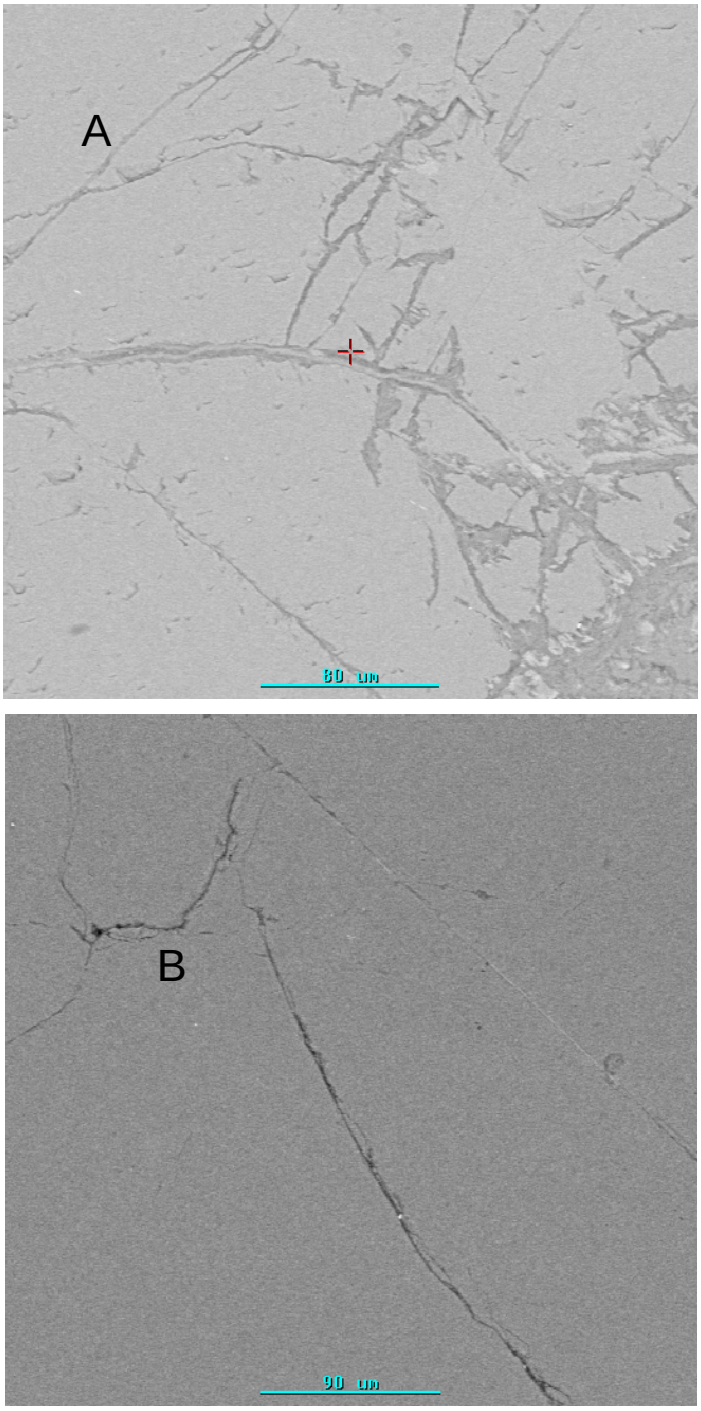

Figure A1 5 SEM image showing microfractures in orthopyroxene (A) and plagioclase (B) crystals from Amandelbult

The boundary between the plagioclase and orthopyroxene grains in Figure A1 6 is clearly open (in the Impala 10-shaft sample). Open fractures were also observed within the plagioclase and orthopyroxene crystals. Small laths of biotite

were seen enclosed in the plagioclase and orthopyroxene (centre of Figure A1 6). Small sulphide grains were also observed enclosed in the orthopyroxene and plagioclase and along grain boundaries. The sulphides have been identified as pyrite, pyrrhotite, pentlandite and chalcopyrite.

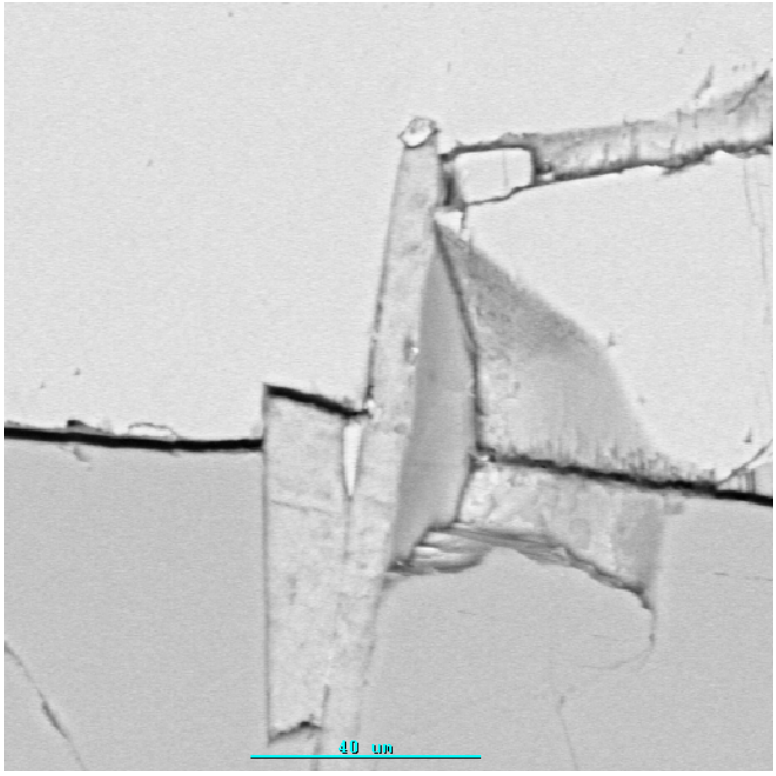

Figure A1 6 The boundary between the plagioclase (dark grey bottom) and orthopyroxene (top) grains is open in the sample from Impala

A1.5 Discussion

The results of the investigation suggest that the nonlinear stress-strain behaviour of the rock samples from Impala is not the product of mineral type, alignment of crystals or even the presence of microfractures, but rather the degree of fracture openness. Filling observed in some of the fractures show that these fractures existed prior to mining or drilling. The literature review highlighted the overall lack of published studies on the controls of rock mass behaviour in Bushveld rocks.

A1.6 Conclusions

The nonlinear stress-strain behaviour of the Impala rocks appears to be as a result of open micro-fractures and not the product of mineral type, alignment of crystals or presence of micro-fractures. While micro-fracturing was observed in all the samples, it appears that the degree of openness of these fractures determines the degree of non-linearity.

A1.7 References

Wilson, A.H., Jermy, C.A. and Ridgeway, M. (2005). Rock-strength and physical properties of norites of the Merensky and Bastard Units, western Bushveld Complex. *S.A. J. of Geology*, Vol.108, pp 525-540.

Kranz, R.L. (1983). Microcracks in rocks: A Review. *Tectonophysics*, Vol.100, pp. 449-480.

Johnson, P.A. and Rasolofosaon, P.N.J. (1996). Nonlinear elasticity and stress-induced anisotropy in rock. *J. Geophysical Research B*: Solid Earth, Vol.101, pp. 3113-3124.

Lyakovsky, V., Reches, Z., Weinberger, R. and Scott, T.E. (1997). Non-linear elastic behaviour of damaged rocks. *Geophysical Journal International*, Vol.130, pp. 157-166.

Li, C., Prikryl, R. and Nordlund, E. (1998). The stress-strain behaviour of rock material related to fracture under compression. *Engineering Geology*, Vol.49, pp. 293-302.

Ryder, J.A. and Jager, A.J. (2002). A textbook on rock mechanics for tabular hard rock mines, The Safety in Mines Research Advisory Committee (SIMRAC), Braamfontein, RSA, pp. 174-278.

Lavrov, A. (2005). Fracture-induced physical phenomena and memory effects in rocks: a review. *Strain*, Vol.41, pp. 135-149.

Hurlbut, C.S. and Klein, C. (1977). Manual of Mineralogy (after James D. Dana). *John Wiley*, New York, pp. 532.

Heinrich, W.W. (1965). Microscopic identification of minerals. *McGraw-Hill*, New York, pp. 414.

Bucur, V. and Rasolofosaon, P.N.J. (1998). Dynamic elastic anisotropy and nonlinearity in wood and rock. *Ultrasonics*, Vol.36, pp. 813-824.

A2 Detailed XRF investigation

A2.1 Major elements (wt %)

Table A2 1 Major elements (wt %) determined for the samples from Amandelbult (J0124 – J0126), Union (J0123) and Impala (J0115 – J0122 & J0127)

Sample	SiO_2	TiO_2	Al_2O_3	Fe_2O_3(t)	MnO	MgO	CaO	Na_2O	K_2O	P_2O_5	Cr_2O_3	L.O.I.	Total	H_2O^-
J0115	48.53	0.09	27.98	2.65	0.042	3.08	15.18	1.87	0.17	0.018	0.035	-0.10	99.53	0.12
J0116	48.65	0.10	26.35	3.32	0.056	4.10	15.09	1.68	0.16	0.017	0.053	-0.11	99.48	0.11
J0117	49.76	0.14	19.21	6.70	0.111	10.05	11.68	1.50	0.11	0.014	0.143	-0.17	99.24	0.10
J0118	53.18	0.24	5.46	12.24	0.207	22.64	4.44	0.28	0.21	0.283	0.366	-0.14	99.41	0.10
J0119	47.73	0.08	29.87	1.76	0.026	1.26	16.32	2.27	0.15	0.017	0.008	0.05	99.55	0.17
J0120	48.27	0.10	27.01	2.99	0.050	3.48	15.33	2.13	0.17	0.016	0.043	-0.08	99.51	0.23
J0121	48.45	0.09	27.01	2.93	0.047	3.67	15.02	2.04	0.17	0.018	0.045	0.04	99.52	0.06
J0122	52.83	0.23	7.32	11.10	0.192	21.11	5.81	0.49	0.18	0.030	0.360	-0.31	99.35	0.23
J0123	50.98	0.14	13.86	8.14	0.149	15.51	8.91	0.98	0.08	0.012	0.255	0.30	99.30	0.14
J0124	47.45	0.08	26.85	3.04	0.050	3.88	15.41	2.03	0.17	0.016	0.048	0.04	99.05	0.07
J0125	47.03	0.10	18.98	5.80	0.097	9.66	11.93	1.35	0.14	0.012	0.149	3.96	99.21	0.16
J0126	53.19	0.25	5.18	12.26	0.217	22.58	4.75	0.27	0.24	0.058	0.371	-0.15	99.22	0.09
J0127	52.06	0.17	6.89	12.84	0.220	20.49	6.01	0.36	0.06	0.014	0.404	-0.14	99.38	0.04

A2.2 Trace elements (ppm)

Table A2 2 Trace elements from Amandelbult (J0124 – J0126), Union (J0123) and Impala (J0115 – J0122 & J0127)

Sample	As	Ba	Bi	Br	Ce	Co	Cr	Cs	Cu	Ga	Ge	Hf	La
J0115	<4	88	<3	<2	<10	12	254	<5	56	19	<1	<3	<10
J0116	<4	69	<3	<2	<10	17	333	<5	53	16	<1	<3	<10
J0117	<4	67	<3	<2	<10	44	923	<5	231	14	<1	<3	<10
J0118	<4	74	<3	<2	<10	96	2397	<5	722	6.8	1.2	3.6	12
J0119	<4	74	<3	<2	<10	8.1	81	<5	43	19	<1	<3	<10
J0120	<4	78	<3	<2	<10	16	298	<5	55	18	<1	<3	<10
J0121	<4	83	<3	<2	<10	17	308	<5	59	18	<1	<3	<10
J0122	<4	73	<3	<2	<10	85	2364	<5	501	7.9	<1	<3	<10
J0123	<4	51	<3	<2	<10	56	1669	<5	163	11	<1	<3	<10
J0124	<4	76	<3	<2	<10	15	320	<5	42	17	<1	<3	<10
J0125	<4	79	<3	<2	<10	39	1057	<5	96	13	<1	<3	<10
J0126	<4	123	<3	<2	<10	82	2347	<5	160	6.4	<1	<3	<10
J0127	<4	37	<3	<2	<10	107	2431	<5	1212	6.5	<1	3.2	<10
J0115	<2	1.1	<10	121	<2	3.6	<3	<1	<10	357	<2	<3	<3
J0116	<2	1.3	<10	131	<2	3.2	6.0	<1	<10	309	<2	<3	<3
J0117	<2	1.3	<10	518	<2	2.4	11	<1	<10	269	<2	<3	<3
J0118	<2	2.3	14	1570	2.6	9.9	25	1.7	<10	71	<2	<3	<3
J0119	<2	1.4	<10	78	<2	3.4	<3	<1	<10	378	<2	<3	<3
J0120	<2	1.5	<10	126	<2	3.8	3.4	<1	<10	345	<2	<3	<3
J0121	<2	1.3	<10	133	<2	3.5	3.5	<1	<10	349	<2	<3	<3
J0122	<2	2.1	<10	1221	3.1	6.9	24	1.1	<10	97	<2	<3	<3
J0123	<2	<1	<10	553	<2	2.2	16	<1	<10	176	<2	<3	<3
J0124	<2	1.4	<10	123	3.0	4.1	3.9	<1	<10	342	<2	<3	<3
J0125	<2	1.1	<10	361	3.7	4.1	12	<1	<10	250	<2	<3	<3
J0126	<2	2.0	<10	649	3.7	12	28	<1	<10	63	<2	<3	<3
J0127	<2	1.6	<10	2214	5.1	2.7	27	3.1	<10	82	<2	<3	<3

Trace elements continued (ppm) - Amandelbult (J0124 – J0126), Union (J0123) and Impala (J0115 – J0122 & J0127)

Sample	U	V	W	Y	Yb	Zn	Zr
J0115	<2	28	<3	1.8	<2	16	5.7
J0116	<2	34	<3	2.4	<2	19	7.4
J0117	<2	66	<3	3.2	<2	41	5.5
J0118	<2	118	<3	9.2	<2	77	17
J0119	<2	21	<3	1.2	2.4	11	4.6
J0120	<2	33	<3	2.5	2.3	19	7.6
J0121	<2	32	<3	2.0	<2	19	6.0
J0122	<2	117	<3	6.3	<2	73	17
J0123	<2	83	<3	3.4	2.5	58	5.4
J0124	2.7	28	<3	1.3	<2	15	5.9
J0125	<2	58	<3	2.2	<2	32	3.3
J0126	<2	127	<3	6.8	<2	77	16
J0127	<2	112	<3	3.3	<2	84	8.0

A3 Individual microscopic investigations

A3.1 Amandelbult

A3.1.1 Sample: J0124

Borehole and sample details: Vertical borehole drilled above the panel centre. Sample retrieved at 11.56 m above the stope.

Mining rock name: White spotted anorthosite

IUGS rock name: Leuconorite

Modal proportions: Plagioclase 85 %; Orthopyroxene 12 %; Clinopyroxene < 2 %; Biotite < 1 %; magnetite < 1 %

Texture: The rock has a coarse-grained igneous texture of interlocking crystals. There is no preferred alignment of the plagioclase crystals. The orthopyroxene crystals form isolated interstitial “spots” within the plagioclase.

Fractures: There is no overall orientation of the fractures either parallel or perpendicular to bedding (Figure A3 1 and Figure A3 2). Fractures are short and do not extend beyond two to three crystal lattices. Fractures in plagioclase are controlled by the orientation of their crystal lattices. Fractures cut across plagioclase crystals are orientated approximately 90° to the crystal long axes. Therefore, as the crystal orientation change, so do the fracture orientations. In addition, fractures often terminate along crystal boundaries. The fracture orientation in the interstitial pyroxene generally has a dominant preferred orientation which may be related to the cleavage orientations. The orientations of the fractures in the pyroxenes are therefore also a function of crystal orientation.

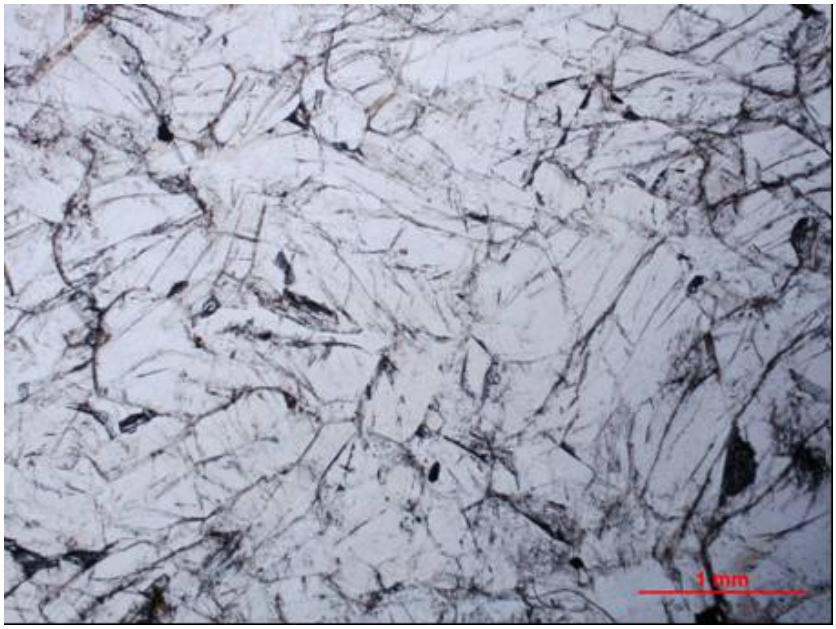

Figure A3 1 Photomicrograph of sample J0124 showing fracturing in plagioclase. There does not appear to be a preferred orientation to the fracturing and fractures do not appear to be laterally extensive (plane polarised light – ppl).

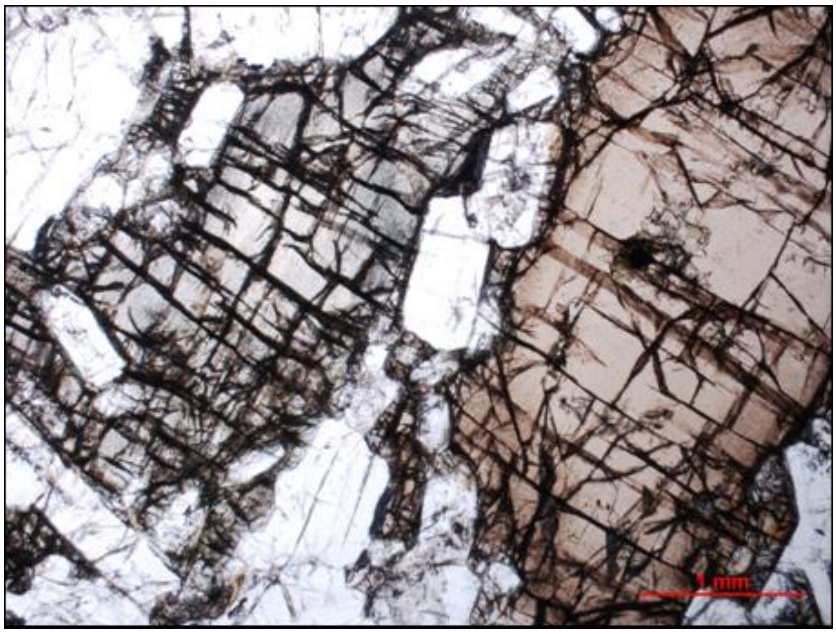

Figure A3 2 Photomicrograph of sample J0124 showing fracturing in plagioclase. There does not appear to be a preferred orientation to the fracturing and fractures do not appear to be laterally extensive (plane polarised light – ppl)

A3.1.2 Sample: J0125

Borehole and sample details: 13-16W – 5E Vertical borehole at centre of panel. Sample retrieved at 5.56 m above the stope.

Mining rock name: Norite

IUGS rock name: Norite

Modal proportions: Plagioclase 50 %; Orthopyroxene 45 %; Clinopyroxene < 2 %; Magnetite <1 %; Biotite < 1 %

Textures: The rock has a very coarse-grained igneous texture of interlocking crystals. The rock is dominated by plagioclase with lesser amounts of orthopyroxene. There is no preferred orientation of the plagioclase crystals. The orthopyroxene crystals have possible preferred orientation although this is only evident from the cleavage patterns.

Fractures: This sample is highly fractured (Figure A3 3). Fractures appear to extend in many directions but are dominated by extensive, long fractures in a single orientation. These fractures are prevalent in the plagioclase crystals although also evident in the pyroxene crystals. The pyroxene crystals are marginally altered especially along the fractures.

Figure A3 3 Photomicrograph of sample J0125 showing fracturing in plagioclase. The fractures have a preferred orientation from left to right across the image. It is suggested that these fractures have been accentuated by the thin section preparation process (ppl)

A3.1.3 Sample: J0126

Borehole and sample details: Horizontal borehole drilled over Pillar 3 (P3-6.5 m) 2509-UCM-09

Mining rock name: Pyroxenite

IUGS rock name: Melanorite

Modal proportions: Plagioclase 15 %; Orthopyroxene 82 %; Biotite 2 %; Magnetite < 1%

Textures: The rock has a very coarse-grained igneous texture of interlocking crystals. The rock is dominated by pyroxene with interstitial plagioclase. Plates of biotite are present in the rock.

Fractures: The orthopyroxene crystals are highly fractured (Figure A3 4 and Figure A3 5). The fractures appear to have a preferred orientation and extend across multiple orthopyroxene crystal boundaries. The fractures cut into the interstitial plagioclase but are often terminated and do not extend across the whole plagioclase area. The fractures in the orthopyroxene crystals are most likely related to the cleavage planes suggesting that the crystals themselves are similarly orientated.

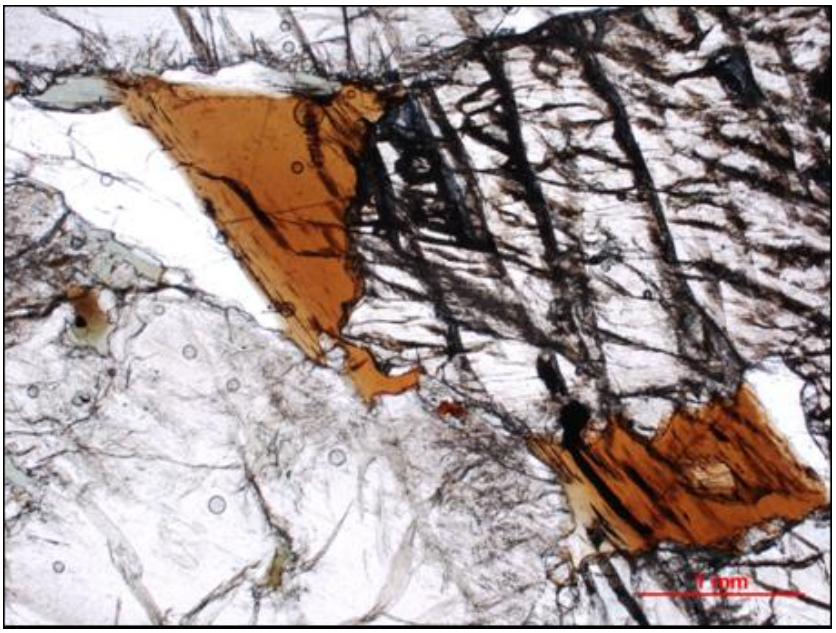

Figure A3 4 Photomicrograph of sample J0126 showing fracturing in orthopyroxene. The fractures are accentuated by the high relief of pyroxene (relative to plagioclase) when the thin section is viewed through transmitted light. Biotite (brown mineral) is also present (ppl)

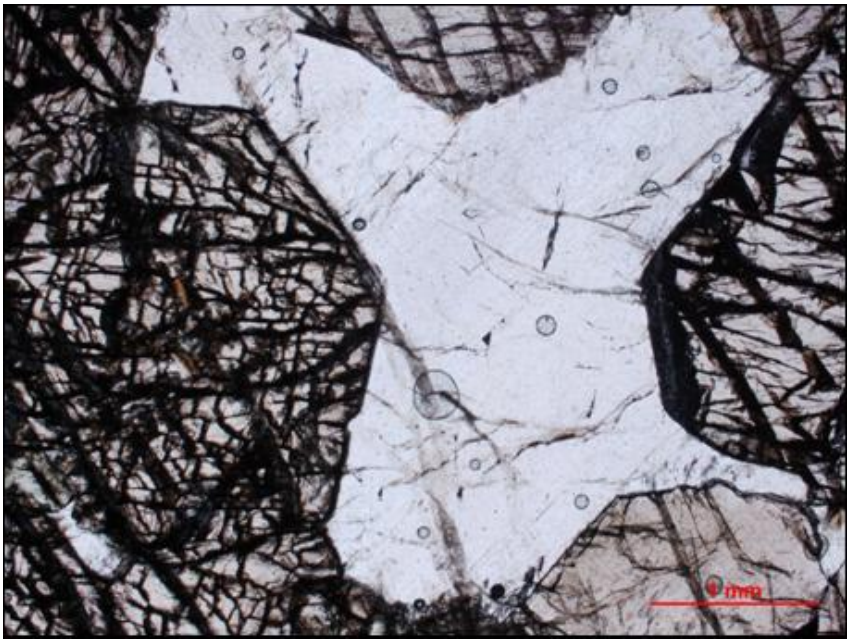

Figure A3 5 Photomicrograph of sample J0126 showing fracturing in orthopyroxene. The fractures from the orthopyroxene do not extend into the interstitial plagioclase (ppl)

A3.2 Impala 10 shaft

A3.2.1 Sample J115

Borehole and sample details: Horizontal borehole drilled above Pillar 3 (P3_14.670m)

Mining rock name: White spotted anorthosite

IUGS rock name: Leuco norite

Modal proportions: Plagioclase (PL) 85 %; Orthopyroxene (OPX) 10 %; Clinopyroxene <5 %; Other <5 %

Texture: Long axes of large plagioclase crystals have a preferred orientation through range of approximately 20 ° on other side of a central axis (Figure 1). This is evident in the thin sections cut perpendicular to layering but not in those cut parallel to the layering. This may be a result of stacking of plagioclase crystals against each other resulting in imbrication due to the magma's flow. Orthopyroxene forms plates which are mostly free of plagioclase except along the crystal edges. This results in the "spotty" nature of the rock (Figure 2). Clinopyroxene is a minor interstitial phase. Overall texture is an interlocking igneous texture.

Fractures: There is no overall orientation of fracturing. Fracture pattern and density in orthopyroxene is different to that found in plagioclase. This suggests that the fracturing is largely mineralogically controlled. Fracturing in orthopyroxene is blocky with a dominant orientation and a minor irregular orientation (Figure A3 6 and Figure A3 7). Where excessive fracturing of orthopyroxene occurs, it is most often associated with removal of the pyroxene from the thin section by the grinding process (Figure A3 8). These highly fractured pyroxenes are therefore not considered to be indicative of the stress field of the rock. The plagioclase contains fine fractures that are predominantly confined to individual crystals (Figure A3 9 to Figure A3 12). The fractures fall within a 90 ° angle which is bisected by the perpendicular to the long axis of the individual plagioclase crystals. Where fractures pass through crystal boundaries, they may deflect as they enter a new crystal lattice. The same is true of fractures across twin planes within a plagioclase crystal (Figure A3 13). The longest fractures are less than 5 mm in length and these are never straight but curve as they are deflected through adjacent plagioclase crystals with differing

orientations. The fracture density is approximately 5 fractures per mm, where the fractures are < 0.01 mm in width.

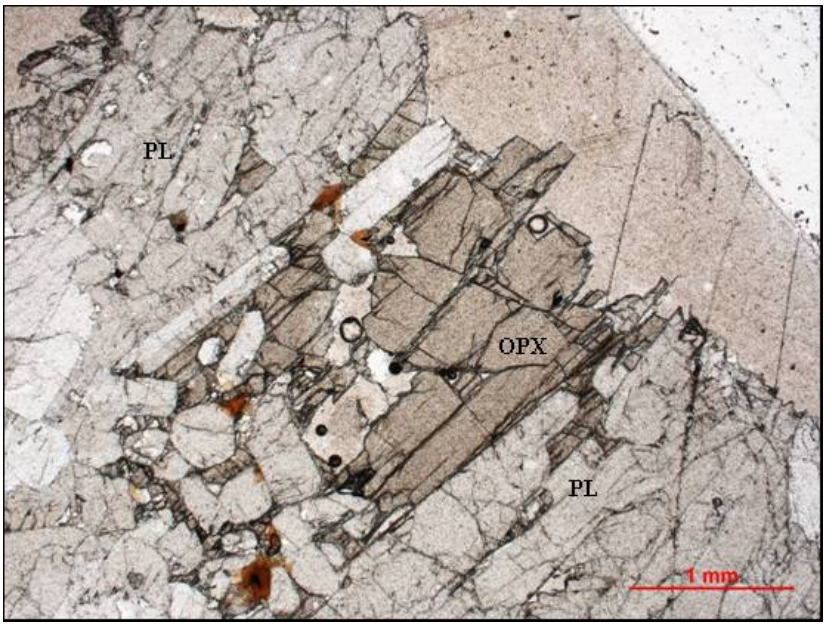

Figure A3 6 Sample J115 Perpendicular to layering "Spot" of orthopyroxene surrounded by plagioclase crystals in the White Spotty Anorthosite.

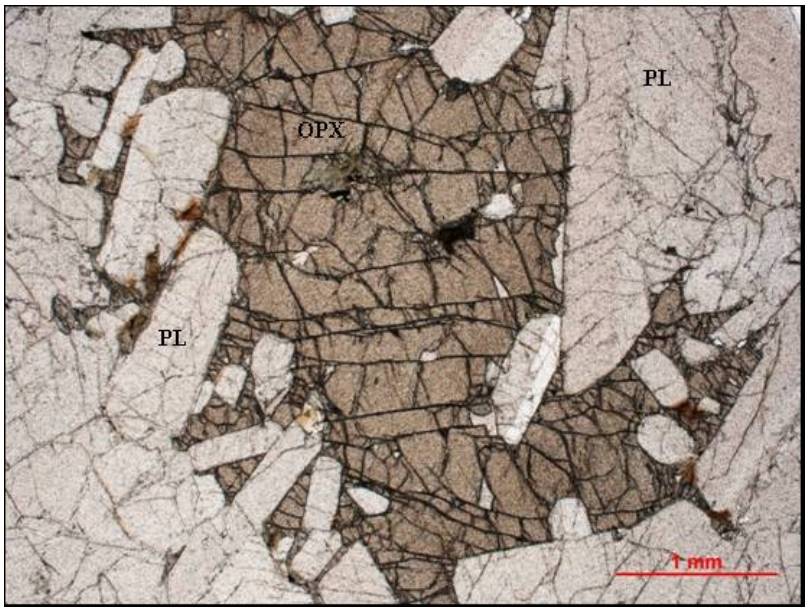

Figure A3 7 Sample J115 Parallel to layering Orthopyroxene "spot" within an interlocking mesh of plagioclase crystals showing two different types of fracturing

Figure A3 8 Sample J115 Perpendicular to layering Very fractured orthopyroxene with central area of orthopyroxene ground away during the sample preparation process

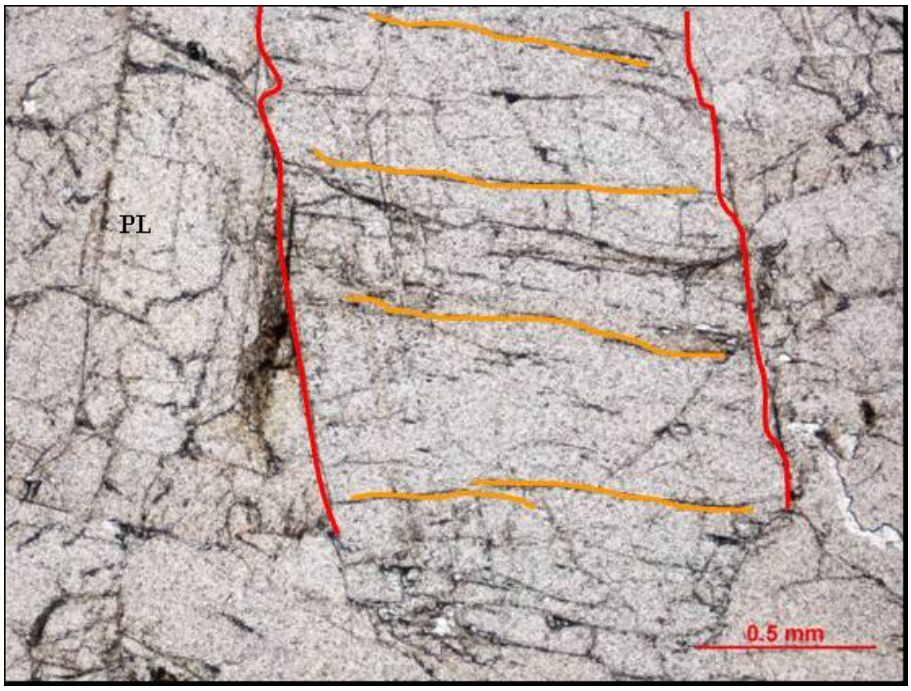

Figure A3 9 Sample J115 Perpendicular to layering Fracturing (in orange) confined to a plagioclase crystal (in red)

Figure A3 10 Sample J115 Perpendicular to layering. There is a lack of orientation in fracturing of plagioclase

Figure A3 11 Sample J115 Parallel to layering. Fracturing in plagioclase is rarely parallel to the long axis of the crystal, but rather between 45 ° either side of the perpendicular (Figure 9)

Figure A3 12 Sample J115 Parallel to layering. Fracture pattern in an area consisting solely of plagioclase is defined by the orientation of the crystals

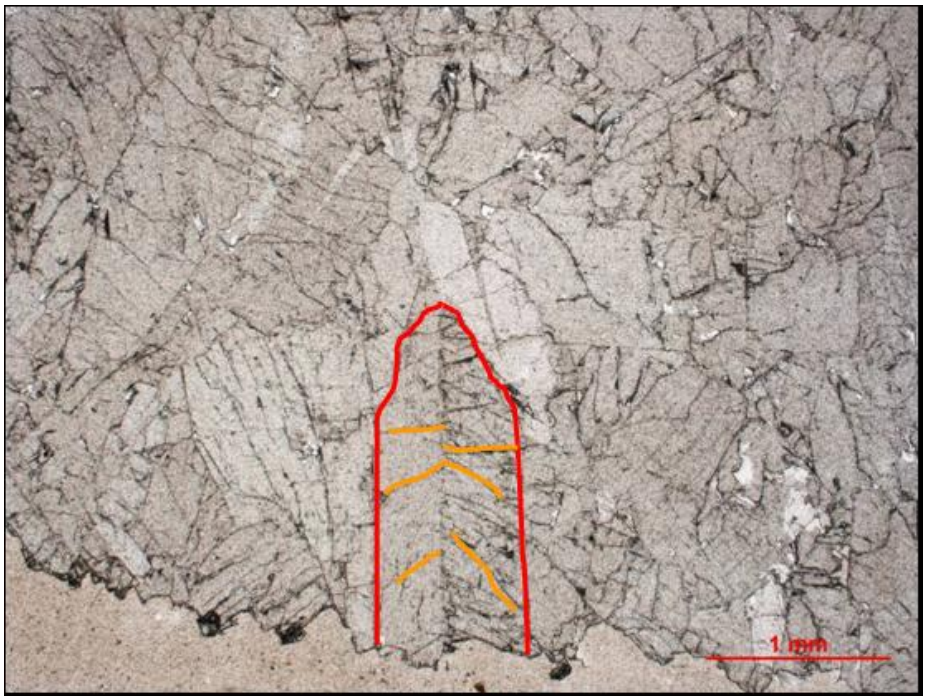

Figure A3 13 Sample J115 Perpendicular to layering. Deflection of fractures (in orange) across a twin plane in a plagioclase crystal (in red)

A3.2.2 Sample J116

Borehole and sample details: Vertical borehole drilled at the centre of the panel. Sample retrieved at 6.57 m above the stope (2545-UCM-12)

Mining rock name: White Spotted Anorthosite

IUGS rock name: Leuco norite

Modal proportions: Plagioclase 85 %; Orthopyroxene 12 %; Clinopyroxene 5 %; Other <3 %

Texture: Preferred orientation of the plagioclase crystals is approximately 20 ° either side of a central axis when viewed in thin sections cut perpendicular to the layering (Figure 11). This is not seen parallel to the layering. This is due to the imbrication of the plagioclase crystals as a result of the flow of the magma. The large orthopyroxene crystals form “spots” within the plagioclase crystal mass. Clinopyroxene is an interstitial phase. The overall texture is an interlocking igneous texture.

Fractures: There is no overall orientation of the fractures evident in thin section. Fracture patterns in orthopyroxene and plagioclase are different. The fracture patterns in orthopyroxene are constrained within the crystal and form a blocky pattern (Figure A3 14 and Figure A3 15). Within this blocky pattern there is a dominant orientation and a lesser irregular orientation. The fracture patterns within the plagioclase crystals is controlled by the crystal orientation where fracturing occurs at right angles to the long axis of the crystals (including zone between 45 ° to either side of perpendicular) (Figure A3 16 and Figure A3 17). While fracturing appears to be confined within each plagioclase crystal, it is evident that fractures do pass through crystal boundaries. When this occurs, the fractures deflect depending on the orientation of the adjacent plagioclase crystal. Fractures may deflect across the twin plane in a plagioclase crystal resulting in a herringbone pattern (Figure A3 18). The longest fractures are less than 5 mm in length and these are never straight but curve as they are deflected through adjacent plagioclase crystals with differing orientations. The fracture density is approximately 5 fractures per mm, where the fractures are < 0.01 mm in width.

Figure A3 14 Sample J116 Perpendicular to layering. Orientation of plagioclase crystals 20 ° either side of a central axis

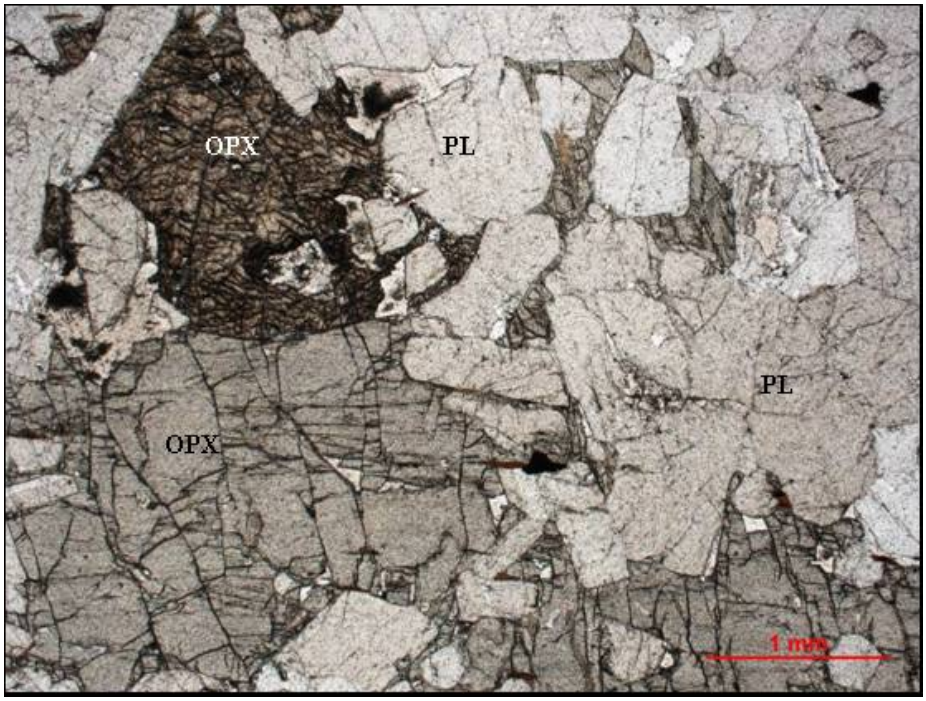

Figure A3 15 Sample J116 Parallel to layering. Fracturing in orthopyroxene has a blocky pattern dominated by fractures in one orientation with lesser irregular fractures in between

Figure A3 16 Sample J116 Perpendicular to layering. Fracturing in plagioclase may pass through crystal boundaries (in red) but tends to deflect as the fractures (in orange) pass from one crystal to another adjacent crystal

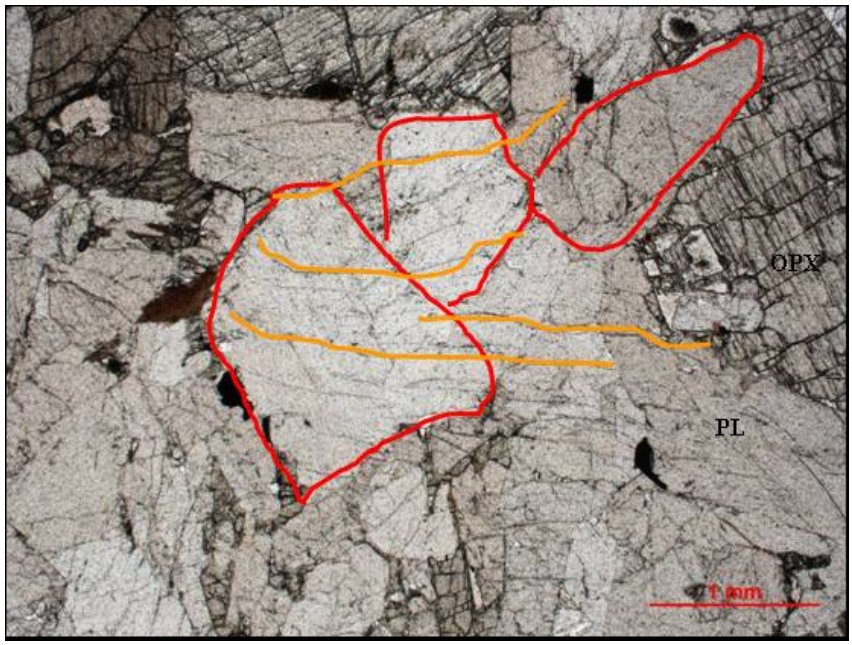

Figure A3 17 Sample J116 Parallel to layering. Fracturing in plagioclase may pass through crystal boundaries (in red) but tends to deflect as the fractures (in orange) pass from one crystal to another adjacent crystal

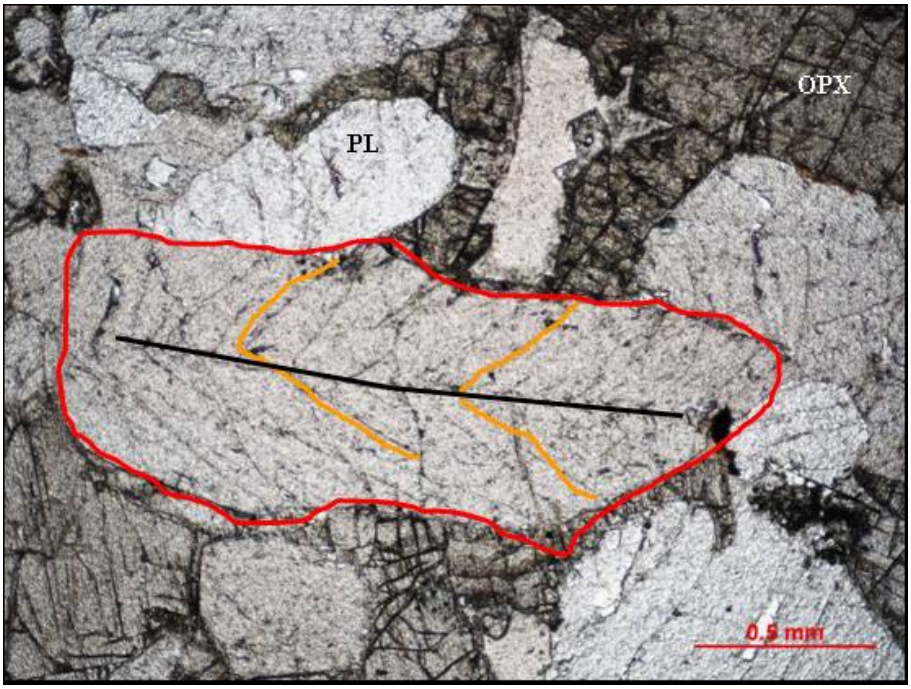

Figure A3 18 Sample J116 Parallel to layering. Herringbone fracture pattern (in orange) across the twin plane (in black) of a plagioclase crystal (in red)

A3.2.3 Sample J117

Borehole and sample details: Vertical borehole drilled at the centre of the panel. Sample retrieved 0.41 m above the stope (2542-UCM-01) Horizontal slide.

Mining rock name: Leuco norite

IUGS rock name: Clinopyroxene norite

Modal proportions: Plagioclase 50 %; Orthopyroxene 40 %; Clinopyroxene 8 %; Other <2 %

Texture: Interlocking igneous texture consisting of plagioclase phenocrysts and orthopyroxene. Poikilitic clinopyroxene is present as a late stage interstitial phase. No orientation of any of the crystals was observed.

Fractures: Fracturing patterns in the orthopyroxene and plagioclase crystals is different. The fracturing within the pyroxene crystals is blocky with a dominant orientation of fractures with irregular fractures in between (Figure A3 19). The dominant fracture orientation appears to be replicated in all the pyroxene crystals. The plagioclase between orthopyroxene crystals does not exhibit this dominant orientation of fracture (Figure A3 20). Where fractures are not confined within individual crystals, they may extend, deflecting through the differently orientated plagioclase crystals, for lengths of up to 5 mm. This has resulted in a series of curved fractures within the predominantly plagioclase areas (Figure A3 19 and Figure A3 21). Fracture patterns in the plagioclase may be confined by crystal boundaries. The orientations of these fractures is controlled by crystal orientation and the cross cutting nature of the fractures. There appears to be more relationships and connectivity in the resultant fracture pattern than has been seen for the other plagioclase dominated rocks. No individual fracture exceeds 7 mm and fracture densities are approximately 4 to 5 fractures (< 0.01 mm wide) per mm.

Figure A3 19 Sample J117 Perpendicular to layering. Differing fracture patterns result in the orthopyroxene crystals and the plagioclase crystals

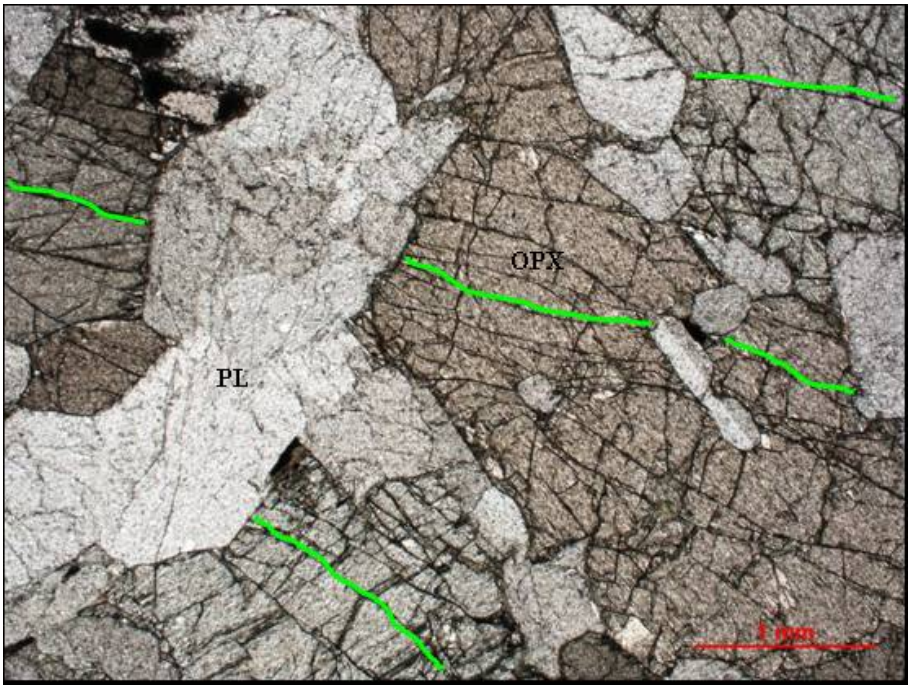

Figure A3 20 Sample J117 Parallel to layering. Fracture patterns (in green) across orthopyroxene grains seem to be orientated, even when the intervening plagioclase does not exhibit any similar fracture pattern

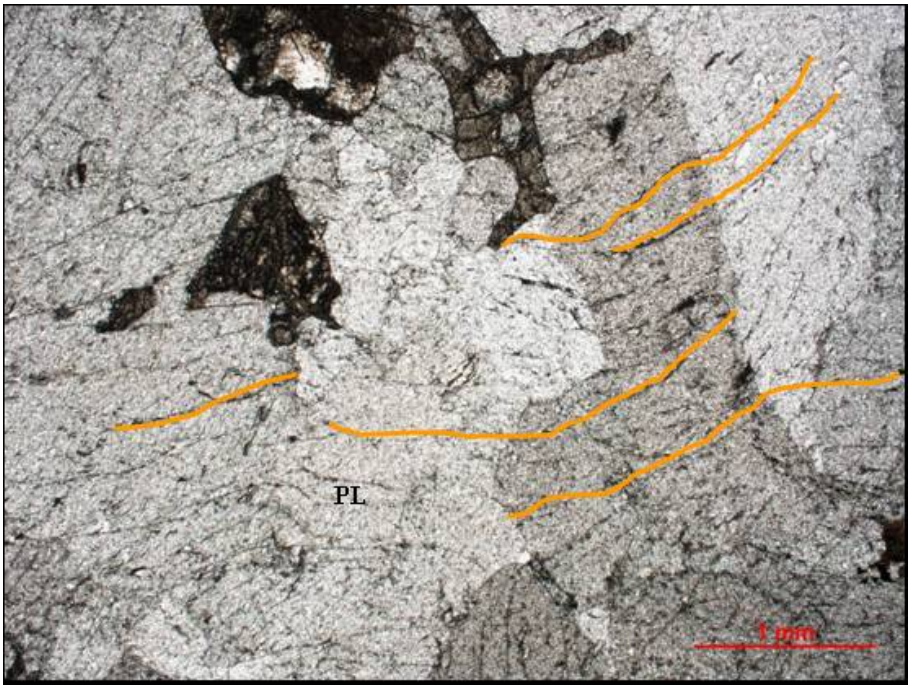

Figure A3 21 Sample J117 Parallel to layering. Curved fracture patterns (in orange) resulting from fractures cross cutting numerous differently orientated plagioclase crystals at right angles

A3.2.4 Sample J118

Borehole and sample details: Vertical borehole drilled adjacent to the abutment in the planned position of Pillar 2.

Mining rock name: Pyroxenite

IUGS rock name: Melanorite

Modal proportions: Plagioclase 15 %; Orthopyroxene 75 %; Clinopyroxene 5 %; Other <5 %

Texture: This rock is dominated by cumulate orthopyroxene with interstitial plagioclase and minor clinopyroxene. The rock has an overall igneous texture of interlocking crystals which do not appear to have a preferred orientation.

Fractures: There appears to be a dominant fracture pattern across the orthopyroxenes, which is poorly transcribed onto the interstitial plagioclase (Figure A3 22 and Figure A3 23a and b). The fracturing in the orthopyroxenes cross cuts the cleavage planes evident in the orthopyroxene crystals. The fracturing in the interstitial plagioclase is generally only related to the dominant fracture orientation of the surrounding orthopyroxenes. The typical fracture features are not dominant here and it can be deduced that this is due to the presence of plagioclase as an interstitial phase and not individual plagioclase phenocrysts. Maximum fracture lengths are 8 mm and fracture densities vary from 2 to 8 fractures (< 0.01 mm wide) per mm.

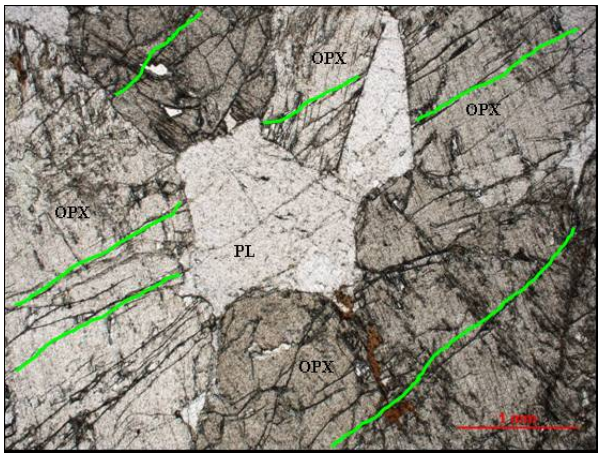

Figure A3 22 Sample J118 Perpendicular to layering. Fracture patterns in the orthopyroxene crystals (in green) show a dominant trend that extends across the whole field of view from bottom left to top right. This dominant trend, while not strongly defined, is still visible in the interstitial plagioclase

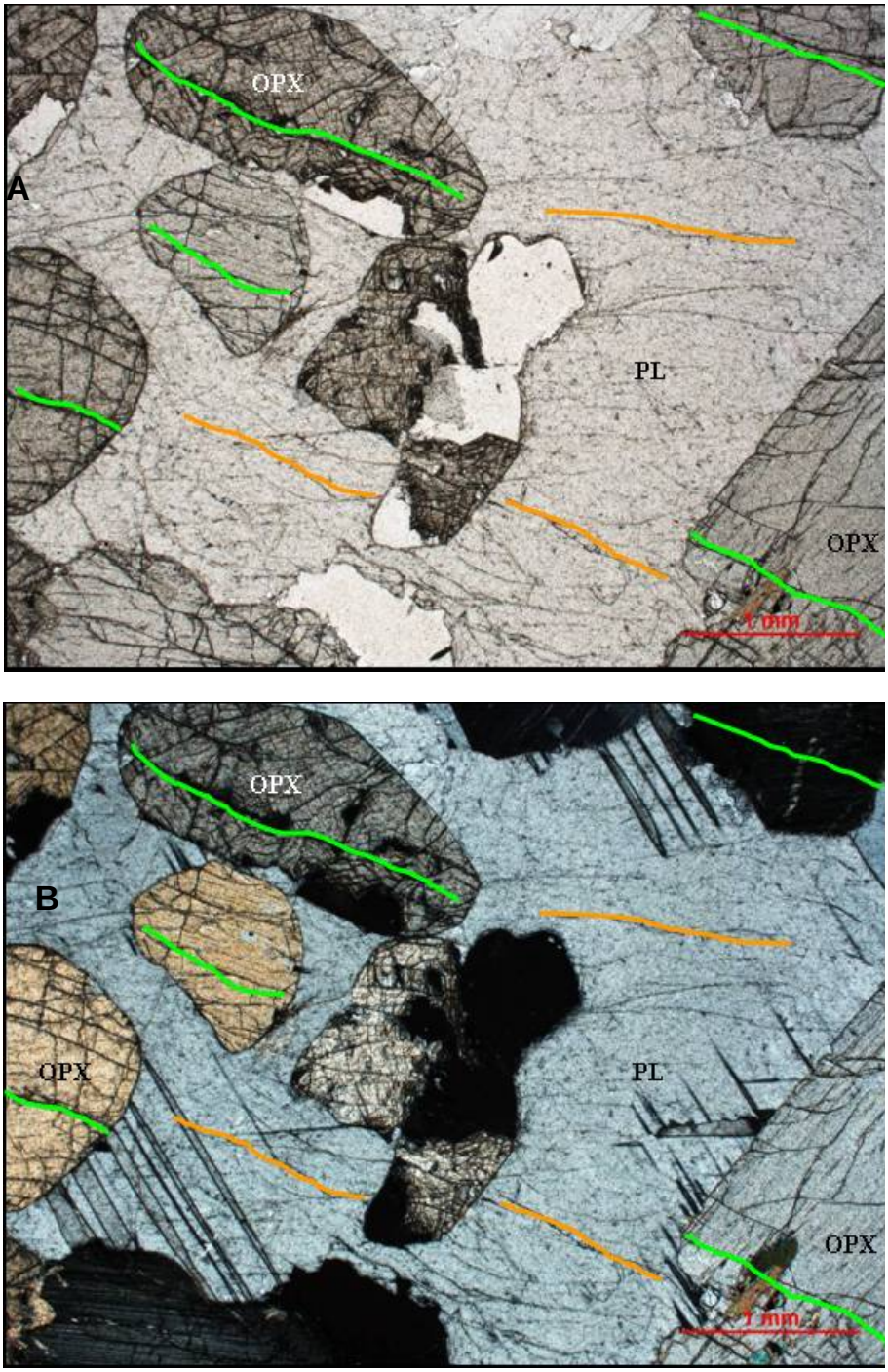

Figure A3 23 Sample J118 Parallel to layering. Fracture patterns in the orthopyroxene crystals (in green) show a dominant trend that extends across the whole field of view from bottom left to top right. This dominant trend is not strongly defined but still visible in the interstitial plagioclase (in orange). A - plane polarised light; B - cross polarised light

A3.2.5 Sample J119

Borehole and sample details: Vertical borehole drilled above the centre of the panel. Sample retrieved at 8.60 m above the stope (UCM-05)

Mining rock name: Pink Mottled Anorthosite

IUGS rock name: Leuco Norite

Modal proportions: Plagioclase 75 %; Orthopyroxene 15 %; Clinopyroxene 5 %; Other <5 %

Texture: Plagioclase phenocrysts with interstitial orthopyroxene form a poikilitic texture resulting in the “mottled” appearance of this rock (Figure 21). The clinopyroxene exists as an interstitial phase. The plagioclase crystals do not have an obvious orientation although localised areas of preferred orientation are noted. There is an overall interlocking igneous texture.

Fractures: The poikilitic orthopyroxenes are well fractured but there does not appear to be any orientation of these fractures (Figure A3 24 to Figure A3 28). There also does not appear to be a relationship between the fractures of the plagioclase crystals and the fractures of the poikilitic orthopyroxene (Figure A3 24 and Figure A3 25). The fracturing of the plagioclase is typical of that seen in the spotted anorthosite samples. Where fractures are continuous across adjacent plagioclase crystals, the fractures often curve as they deflect across the crystal boundaries (Figure A3 26 and Figure A3 27). This is most common in the areas free of orthopyroxene. Generally the fractures through the plagioclase crystals have no specific orientation and are controlled by the orientation of each plagioclase crystal. Fracture density is between 5 and 7 fractures (< 0.01 mm in width) per mm.

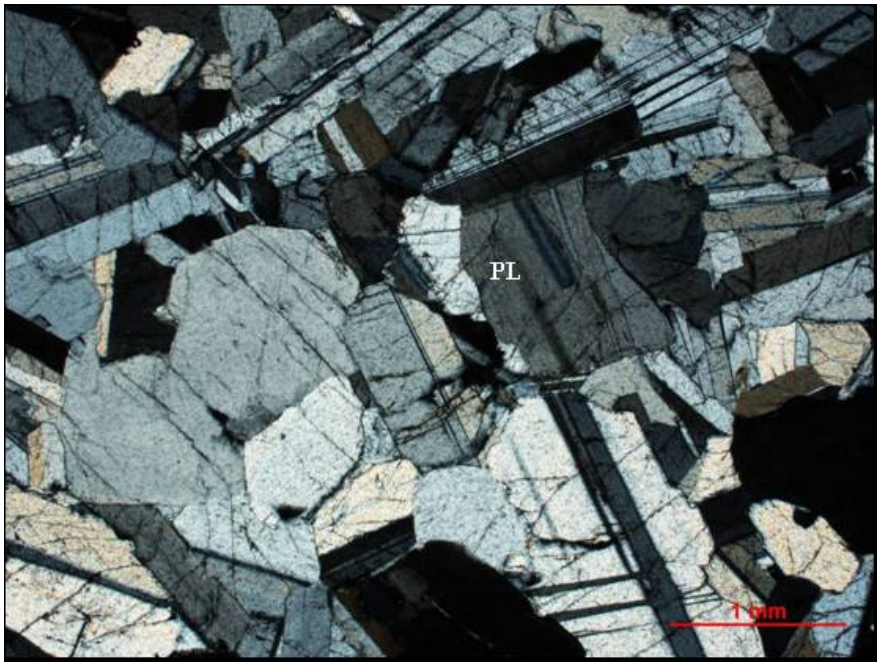

Figure A3 24 Sample J119 Perpendicular to layering. Localised areas of weak alignment of plagioclase crystals

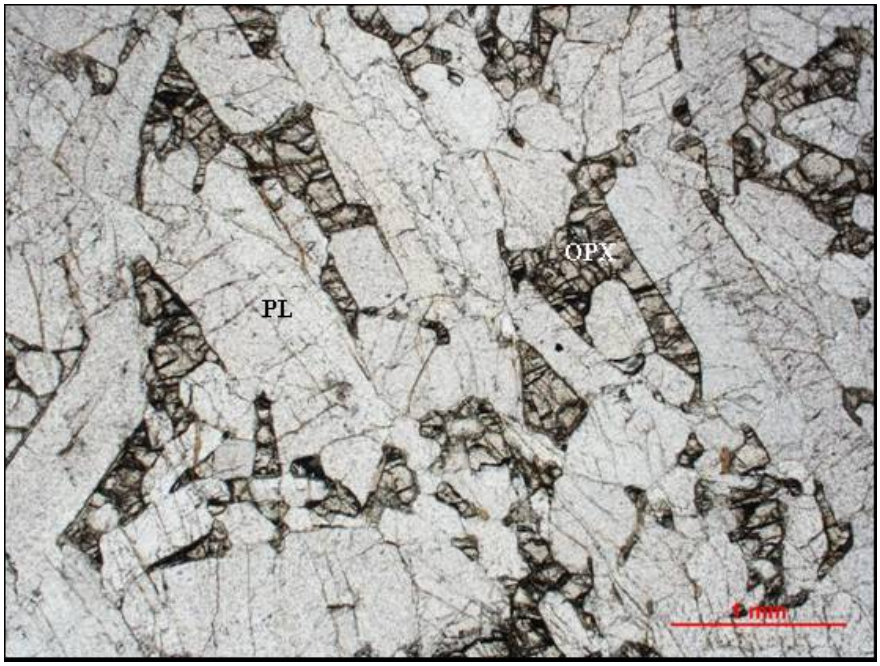

Figure A3 25 Sample J119 Perpendicular to layering. Highly fractured poikilitic orthopyroxene with incorporated plagioclase crystals. There does not appear to be a relationship between the fracturing of the orthopyroxene and the plagioclase

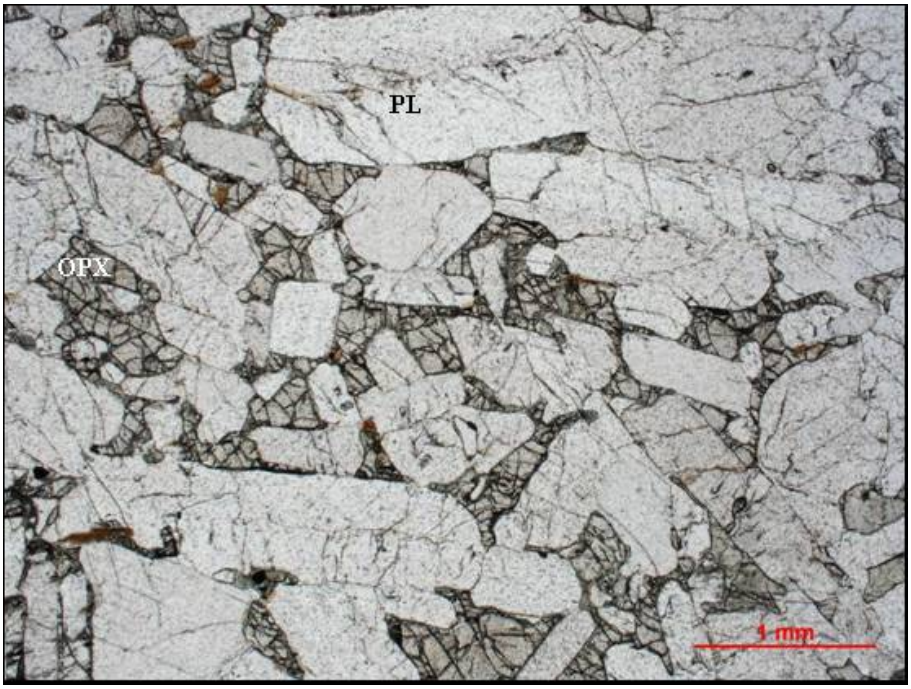

Figure A3 26 Sample J119 Parallel to layering. Highly fractured poikilitic orthopyroxene with differently fractured plagioclase crystals

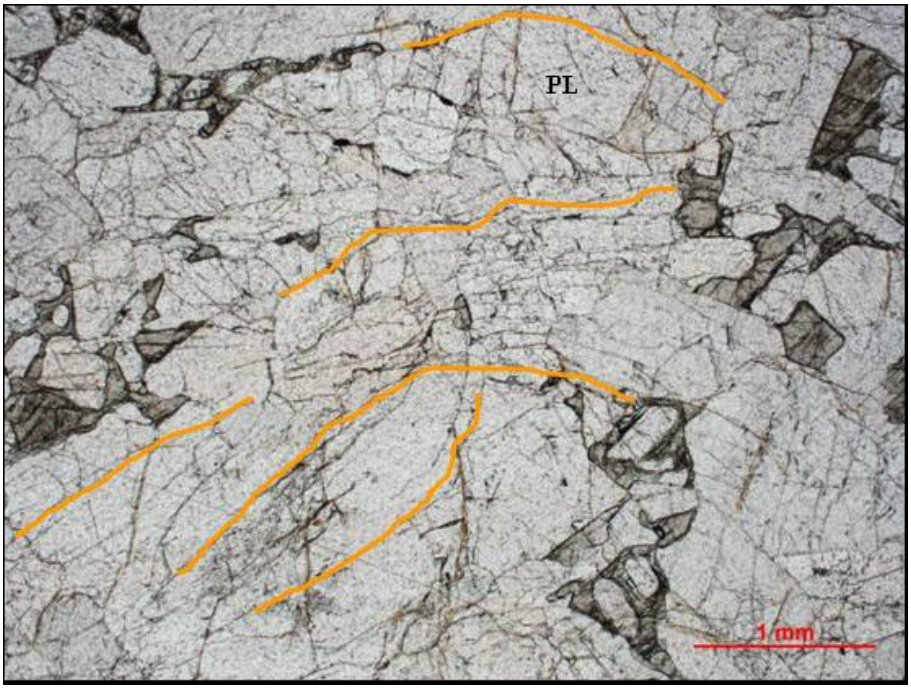

Figure A3 27 Sample J119 Perpendicular to layering. Curved fractures through plagioclase (in orange)

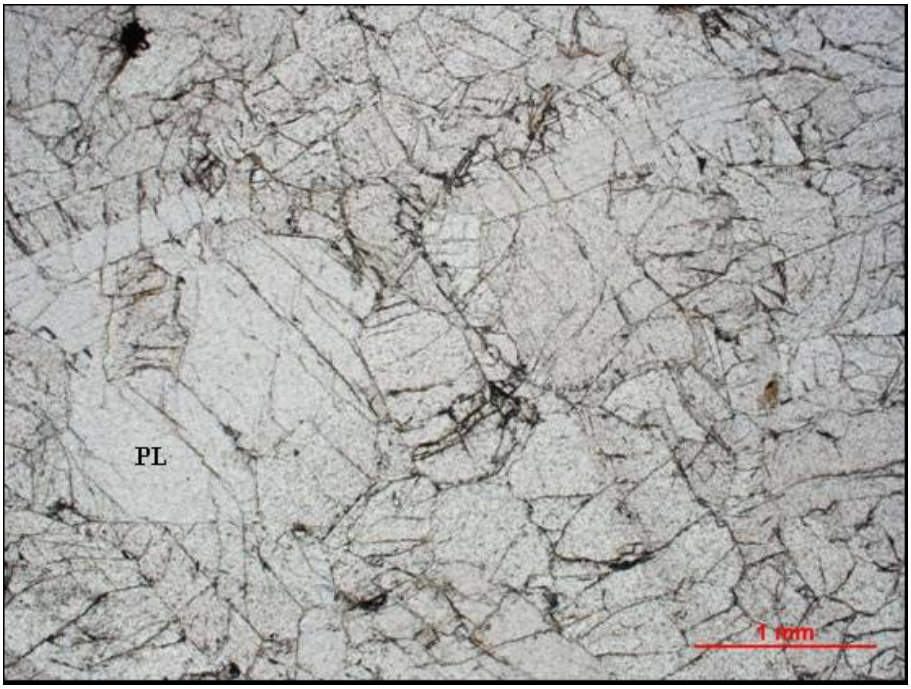

Figure A3 28 Sample J119 Parallel to layering. Fractures in plagioclase do not have any specific orientation but generally cross cut the plagioclase crystals at approximate right angles (Figure B2 13) and deflect at crystal boundaries

A3.2.6 Sample J120

Borehole and sample details: Vertical borehole drilled above the centre of the panel. Sample retrieved at 6.08 m above the stope (2545-UCM-02)

Mining rock name: Pink Spotted Anorthosite

IUGS rock name: Leuco Clinopyroxene Norite

Modal proportions: Plagioclase 65 %; Orthopyroxene 20 %; Clinopyroxene 10 %; Other <5 %

Texture: The rock is dominated by plagioclase with lesser abundances of interstitial orthopyroxene and clinopyroxene. The majority of the orthopyroxene crystals do not have a poikilitic texture and the resultant effect is “spotted” and not “mottled” (Figures 26 and 27). The plagioclase crystals do not have any particular orientation. The overall texture is interlocking crystals forming a typical igneous texture.

Fractures: Orthopyroxene exhibits a dominant fracture orientation with an irregular fracture set in between (Figure A3 29 and Figure A3 30). The plagioclase fractures do not have an overall preferred orientation. The fractures are perpendicular to within 45° of perpendicular to the long axis and are often confined to within an individual crystal (Figure A3 31). A herringbone fracture pattern within a plagioclase crystal may develop where fractures are deflected across a twin plane (Figure A3 32). Deflection of fractures has also occurred where fractures pass through crystal boundaries. This may result in a curved fracture pattern (Figure A3 33). These fractures are rarely greater than 2 mm in length. Clinopyroxene does not appear to be as prone to fracturing as orthopyroxene and plagioclase and as a result does not have a prominent fracture pattern. Fractures are maximum 5 mm in length and are of a density of approximately 5 to 7 fractures (< 0.01 mm wide) per mm.

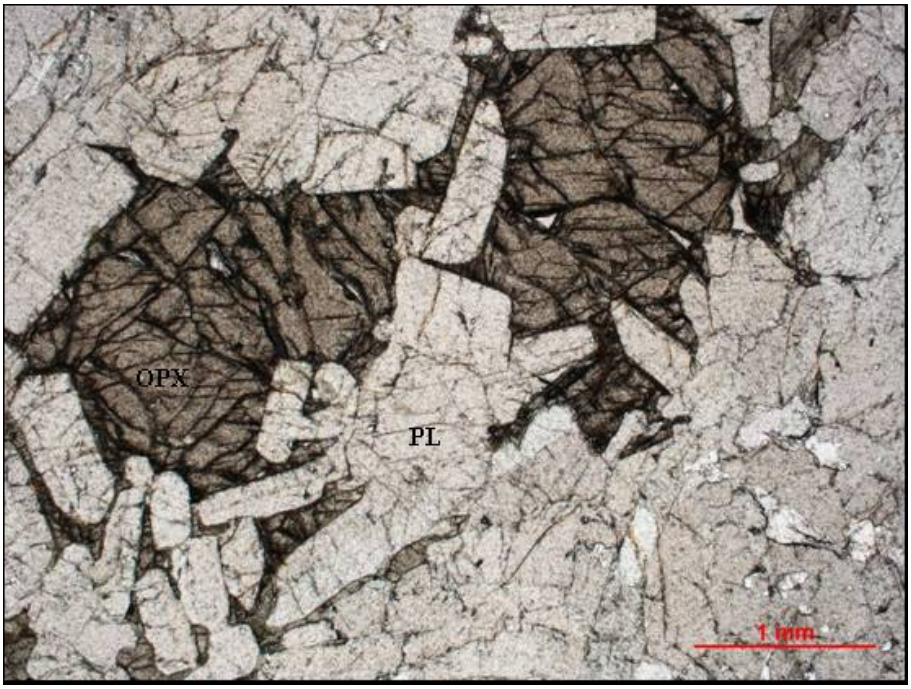

Figure A3 29 Sample J120 Perpendicular to layering. "Spots" of orthopyroxene surrounded by plagioclase crystals

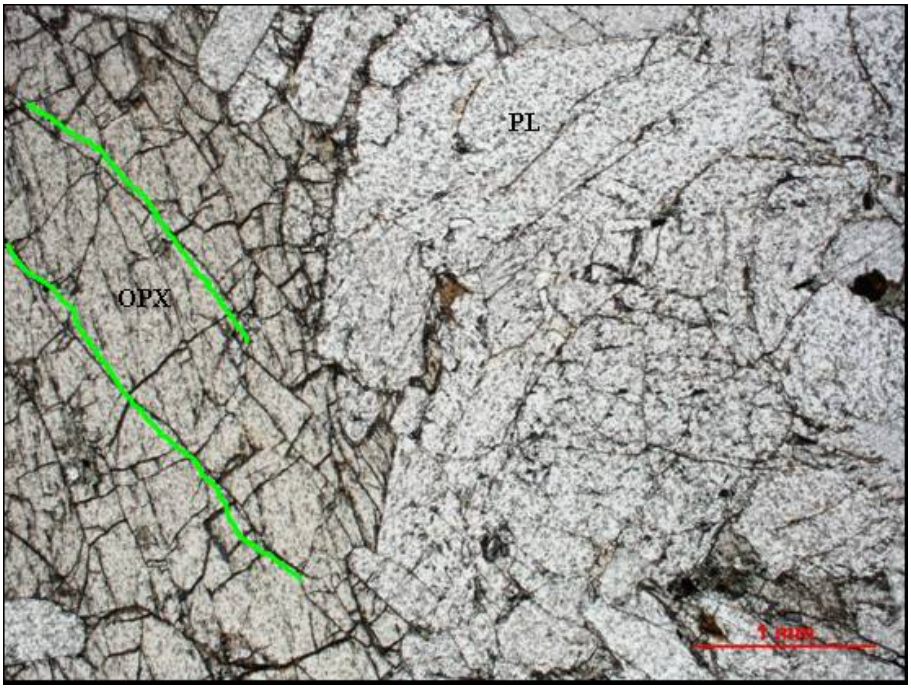

Figure A3 30 Sample J120 Parallel to layering. Fractures in orthopyroxene often have a dominant orientation (in green) with random fracturing joining the dominant fractures

Figure A3 31 Sample J120 Perpendicular to layering. Fractures in plagioclase are controlled by the orientation of the plagioclase crystals (Figure B2 13)

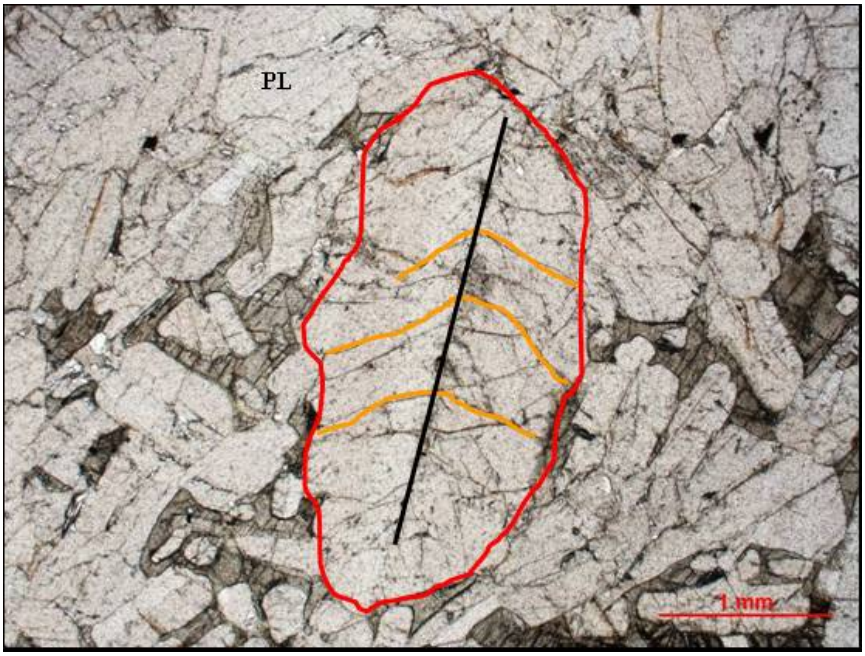

Figure A3 32 Sample J120 Perpendicular to layering. Herringbone fractures (in orange) are caused by fracture deflection across a twin plane (in black) in a plagioclase crystal (in red)

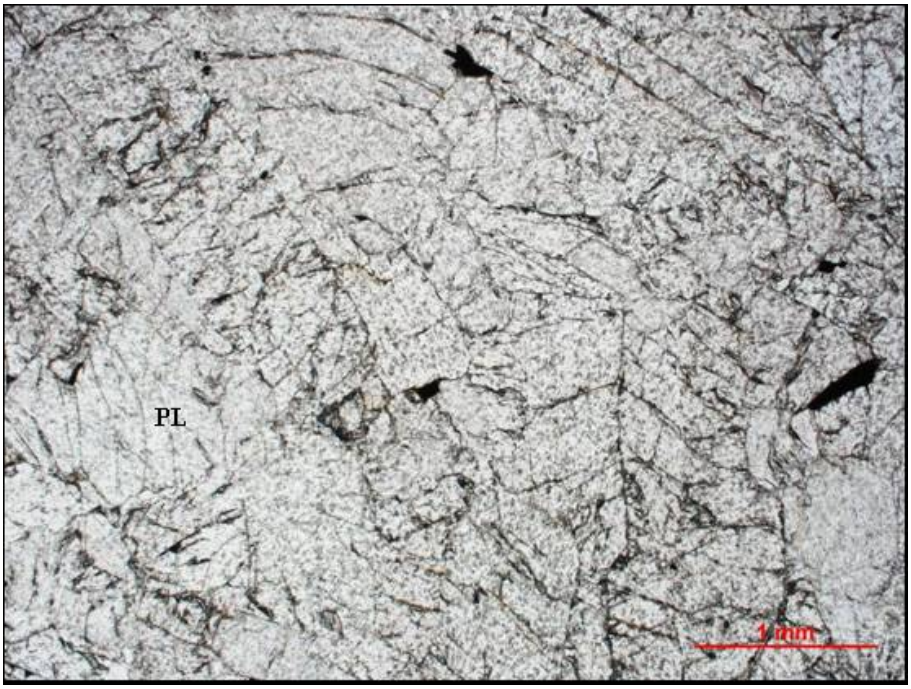

Figure A3 33 Sample J120 Parallel to layering. Fractures in plagioclase do not have any specific orientation but generally cross cut the plagioclase crystals at approximate right angles (Figure B2 13) and deflect at crystal boundaries resulting in curved fracture patterns

A3.2.7 Sample J121

Borehole and sample details: Horizontal borehole drilled over Pillar 1 (2524-UCM-03)

Mining rock name: White Spotted Anorthosite

IUGS rock name: Leuco Norite

Modal proportions: Plagioclase 75 %; Orthopyroxene 15 %; Clinopyroxene 5 %; Other <5 %

This sample was subjected to a compression test.

Texture: This rock is dominated by plagioclase with interstitial orthopyroxene and minor clinopyroxene. There is no preferred orientation of the plagioclase although localised areas where the long axes of the large crystals are aligned are present. The interstitial orthopyroxene contains no plagioclase crystals and forms the “spots” of the Spotted Anorthosite.

Fractures: The fracture patterns of this rock appear to be no different to those observed in the White Spotted Anorthosite that had not been subjected to a compression test. There may be a slightly higher density of fractures but this is difficult to quantify due to the random nature of the fracturing. The fracture patterns in the plagioclase are controlled by the crystal orientation. Fractures are orientated within 45 ° of the perpendicular to the long axis which gives rise to a variety of patterns. Where fractures pass through crystal boundaries or twin planes, they are often deflected resulting in curved fracture patterns or herringbone fractures pattern respectively (Figure A3 34). The fracture patterns in the orthopyroxene crystals are blocky and often at right or near right angles to each other. A dominant fracture orientation is observed in the orthopyroxenes but this does not translate to the plagioclase crystals (Figure A3 35). There is a large abundance of orthopyroxene that has been ground away by the sample preparation process. This may be a factor of an increase in the density of fracturing in the orthopyroxenes. The fractures are not continuous and the maximum length of any fracture is 5 mm with a density of 5 to 8 fractures per mm.

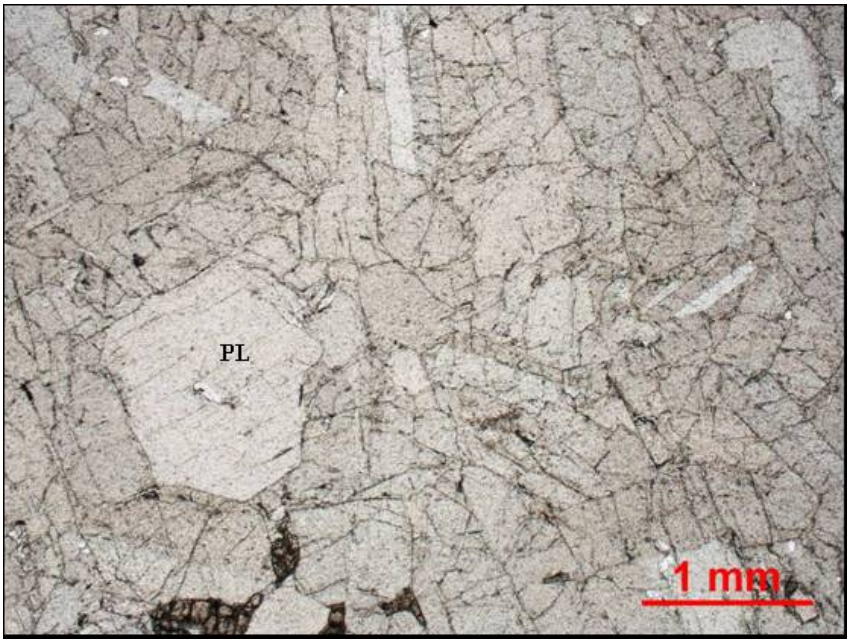

Figure A3 34 Sample J121 Perpendicular to layering. Fractures in plagioclase do not have any specific orientation but generally cross cut the plagioclase crystals at approximate right angles (Figure B2 13) and deflect at crystal boundaries resulting in curved fracture patterns

Figure A3 35 Sample J121 Parallel to layering. Fractures in orthopyroxene are blocky with one dominant orientation translating to all orthopyroxenes which is not reflected strongly in the plagioclase

A3.2.8 Sample J122

Borehole and sample details: Horizontal borehole drilled over Panel 8s (2524-UCM-07)

Mining rock name: Pyroxenite

IUGS rock name: Melanorite

Modal proportions: Plagioclase 20 %; Orthopyroxene 70 %; Clinopyroxene 5 %; Other <5 %

This sample has been subjected to a compression test.

Texture: This rock is dominated by orthopyroxene with interstitial plagioclase and minor clinopyroxene and mica. Interlocking crystals form an overall igneous texture. There is no preferred orientation of the orthopyroxene or plagioclase crystals.

Fractures: This sample has fractures patterns seen in the Pyroxenite (J118) that has not been subjected to any compression tests. The orthopyroxene contains a blocky pattern where a dominant orientated fracture set is prevalent across most of the orthopyroxene crystals (Figure A3 36). Irregular fractures at approximately 90 ° to the dominant fracture set are also present. The interstitial plagioclase does exhibit some patterns, but there is also an imprint of the dominant fracture pattern from the orthopyroxenes (Figure A3 37).

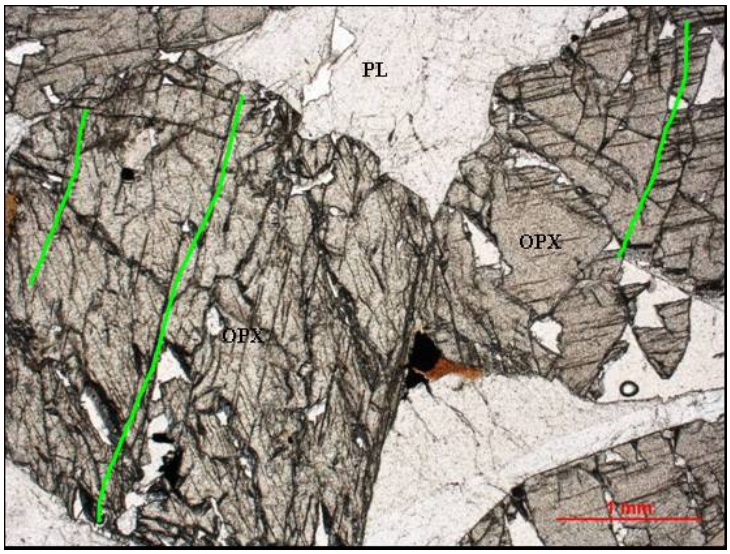

Figure A3 36 Sample J122 Perpendicular to layering. Fractures in orthopyroxene are blocky with one dominant orientation translating to all orthopyroxenes (in green) which is not reflected strongly in the plagioclase

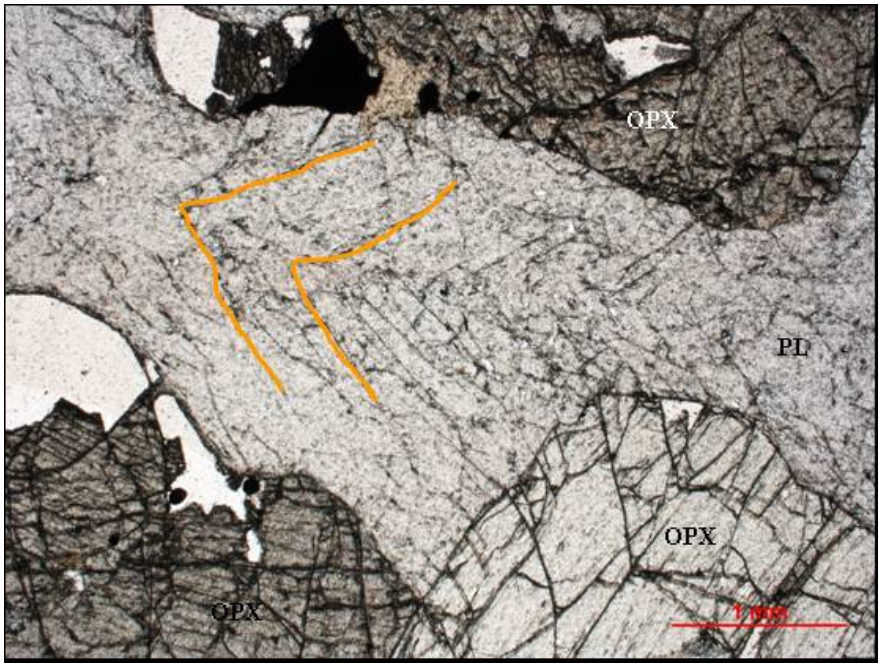

Figure A3 37 Sample J122 Parallel to layering. Herringbone fracture patterns (in orange) in plagioclase as a result of fractures deflected by a twin plane

A3.2.9 Sample: J0127

Borehole and sample details: Vertical borehole drilled adjacent to Pillar 1. Sample retrieved from the Bastard Reef pyroxenite

Mining rock name: Pyroxenite

IUGS rock name: Melanorite

Modal proportions: Plagioclase 15 %; Orthopyroxene 85 %; Biotite <1 %; Magnetite < 1%

Textures: The rock is very coarse-grained and has an igneous texture of interlocking crystals. The rock is dominated by orthopyroxene with lesser interstitial plagioclase. Minor quantities of biotite and magnetite are present.

Fractures: This sample contains abundant fractures in a preferred orientation (Figure A3 38 and Figure A3 39). The fractures dominate the orthopyroxene crystals, and seem to be related to the 90° cleavage of the pyroxene. This suggests that the orthopyroxene crystals have a preferred orientation. These dominant fracture orientations do translate to the plagioclase, although the fractures often terminate within the interstitial plagioclase.

Figure A3 38 Photomicrograph of sample J0127 showing fracturing in plagioclase and orthopyroxene. The fractures in the plagioclase are less pronounced than in the orthopyroxene due to the difference in relief of the two minerals (ppl)

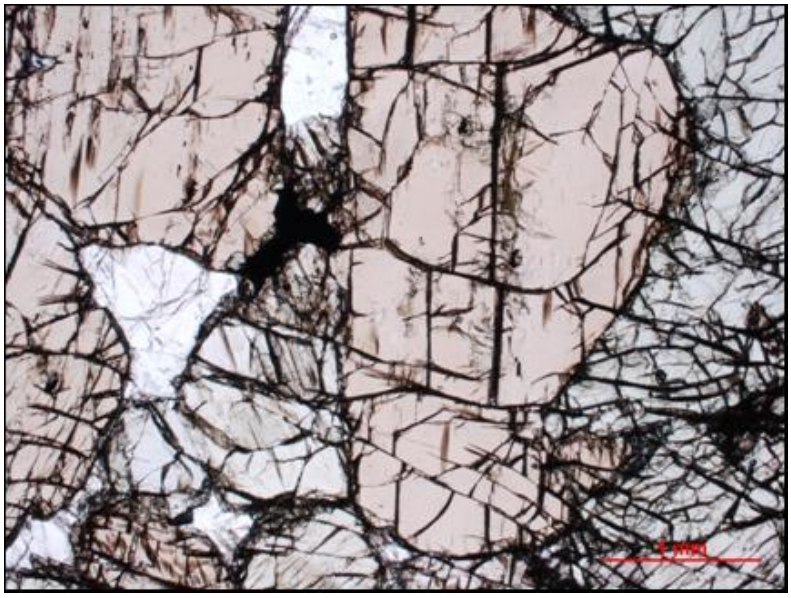

Figure A3 39 Photomicrograph of sample J0127 showing fracturing in orthopyroxene. The fractures extend across the grain boundaries of the orthopyroxene crystals (ppl)

A3.3 Union section

A3.3.1 Sample J123

Borehole and sample details: Horizontal borehole drilled above Pillar 1

Mining rock name: Pyroxenite

IUGS rock name: Melanorite

Modal proportions: Plagioclase 20 %; Orthopyroxene 60 %; Clinopyroxene 10 %; Other <5 %

Textures: The rock contains abundant orthopyroxene with interstitial plagioclase and minor clinopyroxene. Some of the orthopyroxene is poikilitic where the enclosed crystals are plagioclase.

Fractures: In the thin section cut parallel to layering, it is evident that there is a dominant orientation to fractures present in the orthopyroxenes which are only slightly translated to the interstitial plagioclase (Figure A3 40). The orthopyroxene has a far greater fracture density than the plagioclase. The thin sections cut perpendicular to the layering have a prominent preferred orientation of fractures (which therefore are parallel to layering) that is present in both orthopyroxene and the plagioclase (Figure A3 41 and Figure A3 42). These fractures are approximately 0.1 mm apart and have a fracture density of 10 fractures per mm (perpendicular to the fracture orientation). There is a sinuous nature to the fractures. This fracture pattern is distinguishable from all other fracture patterns observed because of the continuity of the fractures across the whole thin section.

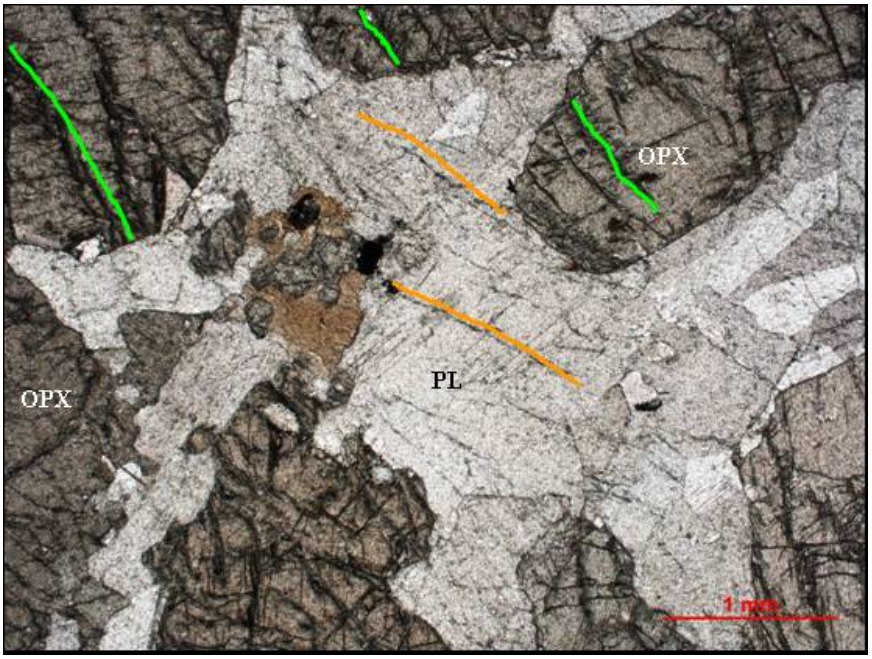

Figure A3 40 Sample J123 Parallel to layering. There is a dominant fracture orientation within the orthopyroxenes which is slightly translated to the interstitial plagioclase

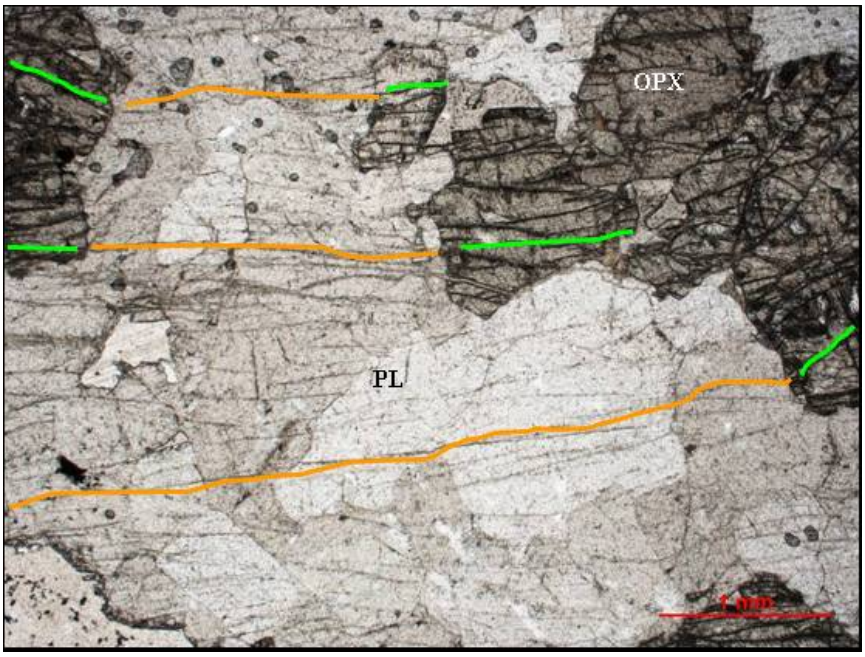

Figure A3 41 Sample J123 Perpendicular to layering. A prominent fracture pattern shows sinuous yet continuous fractures that cut across both the orthopyroxene and the plagioclase crystals

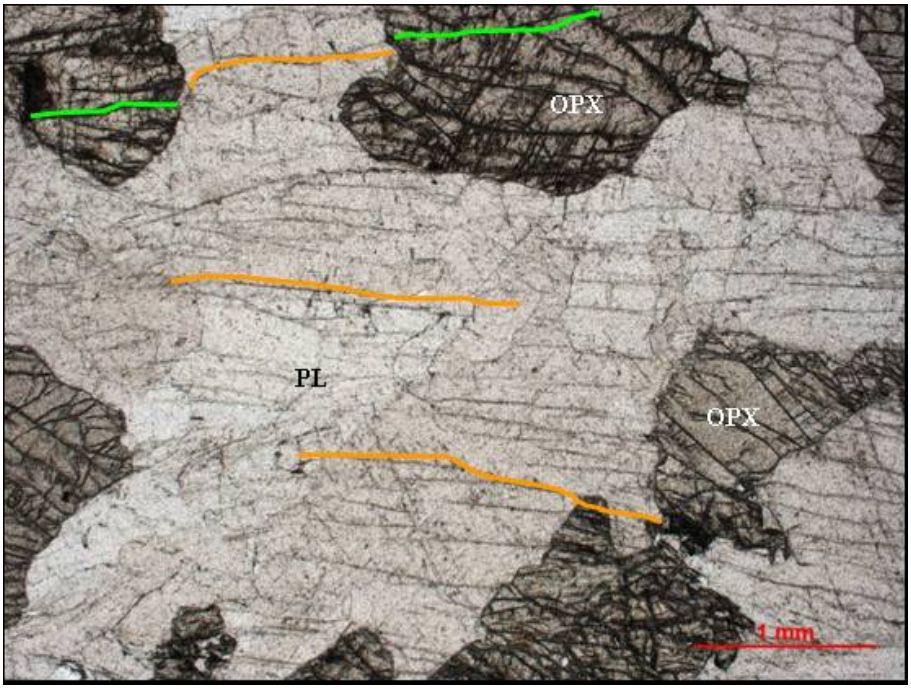

Figure A3 42 Sample J123 Perpendicular to layering. A prominent fracture pattern shows sinuous yet continuous fractures that cut across both the orthopyroxene and the plagioclase crystals

A4 Individual SEM investigations

A4.1 Amandelbult

A4.1.1 Sample J124

In general, the orthopyroxene crystals in Figure A4 1 are more micro-fractured than the plagioclase crystals in Figure A4 2.

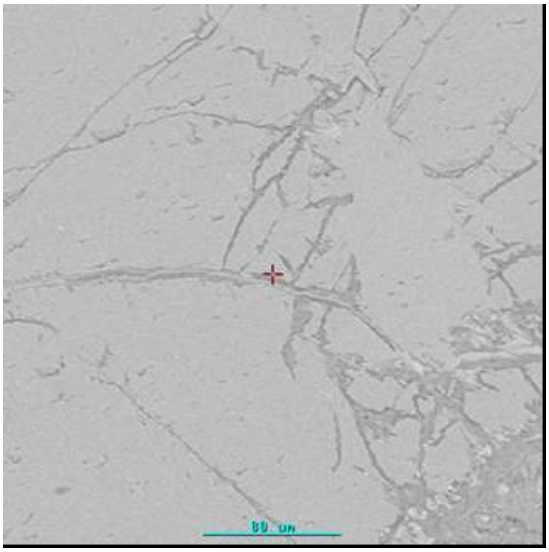

Figure A4 1 SEM image of orthopyroxene crystal showing microfractures

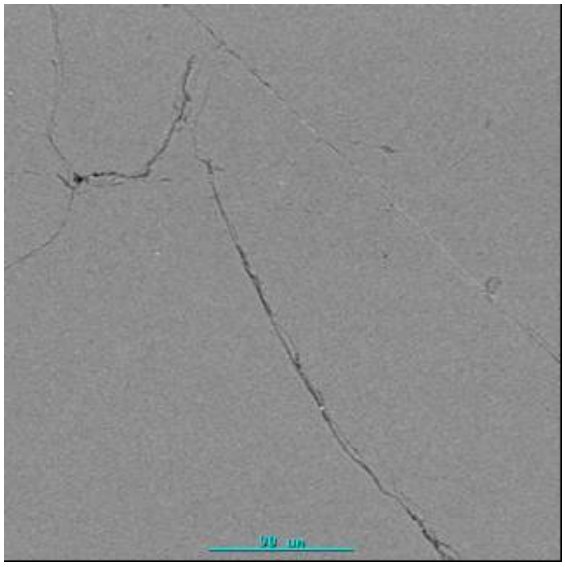

Figure A4 2 SEM image of typical plagioclase crystal. Microfractures are less well developed than in orthopyroxene grains

In both types of minerals, it was difficult to observe conclusively whether the microfractures were open or closed, even under very high magnification. In filled fractures, the fill material had similar compositions to the host mineral (Figure A4 3).

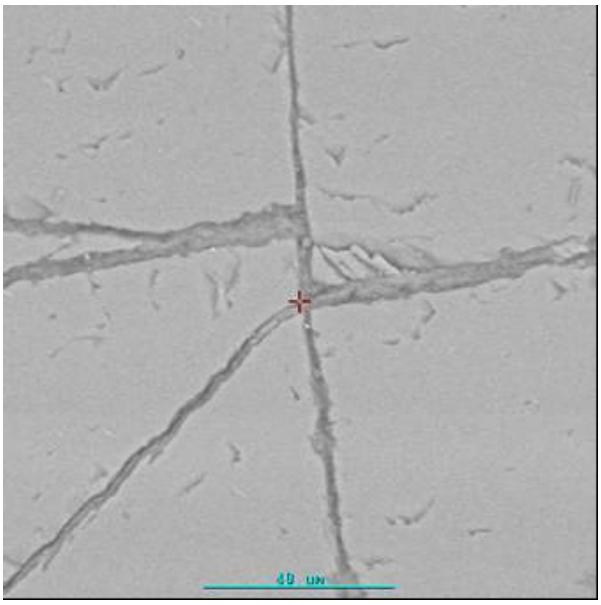

Figure A4 3 Close-up of filled microfractures in orthopyroxene

Small sulphide grains are present in some fractures (Figure A4 4), confirmed by reflected light microscopy of the polished section.

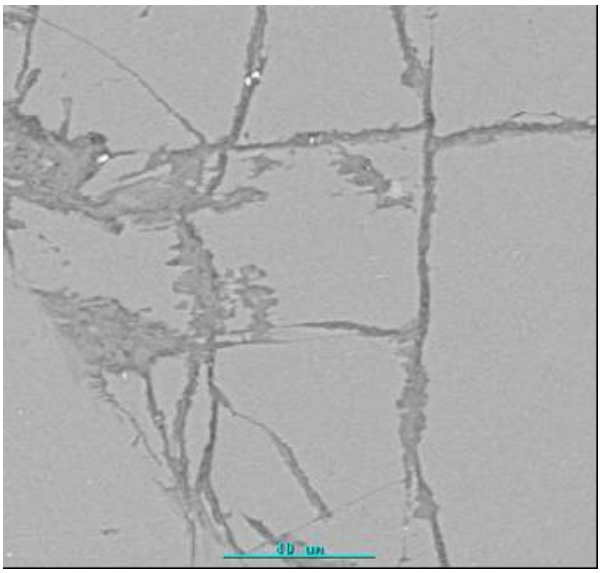

Figure A4 4 SEM image of orthopyroxene grain showing very small sulphide grains (white) in fractures

A4.2 Impala 10-shaft

A4.2.1 Sample J115

It is evident that the orthopyroxene grains were in general more microfractured than the plagioclase grains (Figure A4 5)

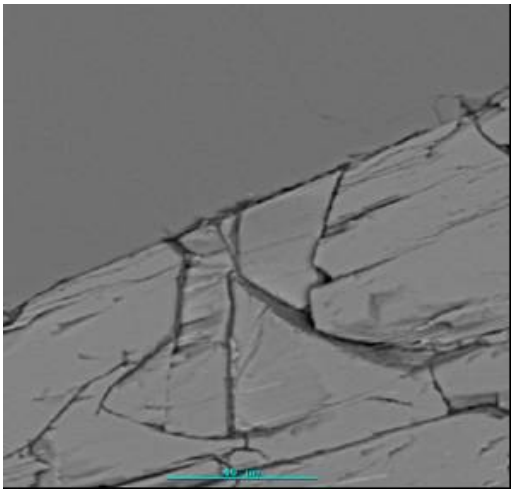

Figure A4 5 Contact between dark grey plagioclase grain (top) and microfractured orthopyroxene grain (light grey) below. The microfractures appear to be open

Both open and filled or partially-filled microfractures were observed. As with the sample from Amandelbult, the fill material appears to be similar to the composition of the host crystal (Figure A4 6). Microfractures also appear to be developed along grain boundaries (Figure A4 7).

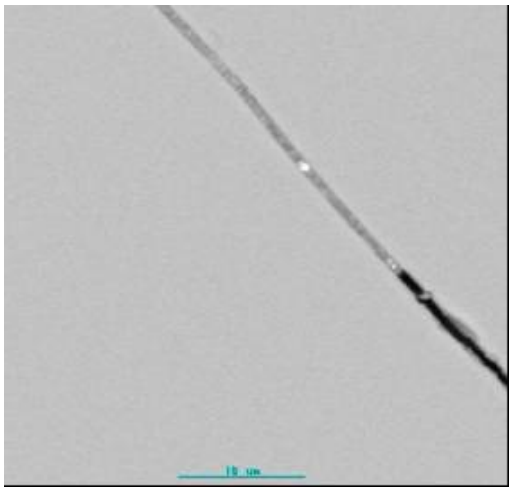

Figure A4 6 Partially-filled microfracture in plagioclase grain. White spot in filled segment is sulphide. Note high magnification

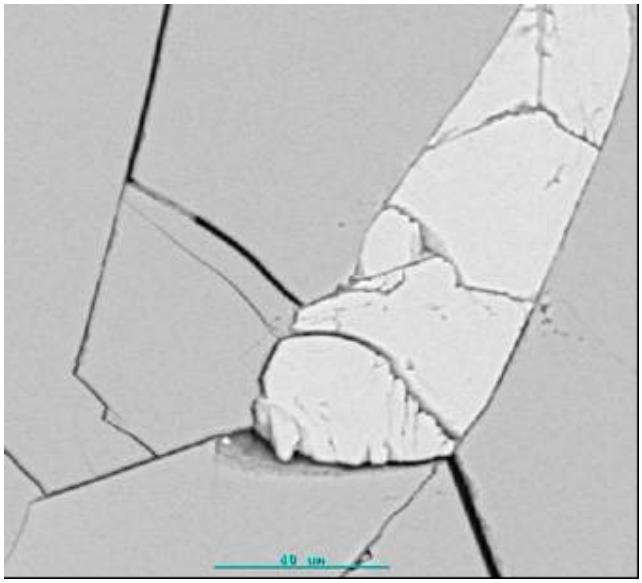

Figure A4 7 Orthopyroxene grain enclosed by darker grey plagioclase grains. The microfractures in the plagioclase appear to be open, with a minor amount of fill along a short segment of the upper-left trending microfracture in the upper left quarter of the image. The irregular microfractures in the orthopyroxene grain also appear to be open

Small laths of biotite enclosed in plagioclase and orthopyroxene were observed in Figure A4 8.

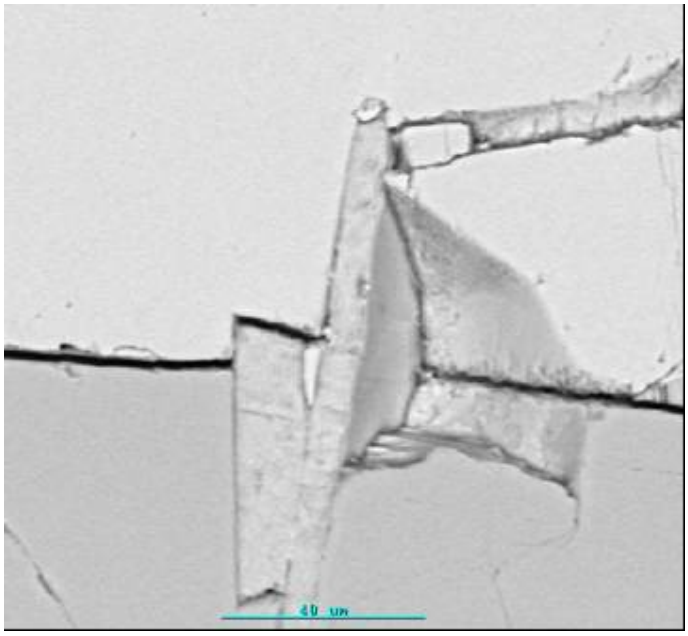

Figure A4 8 Upright laths of biotite in plagioclase (dark grey, bottom) and orthopyroxene (light grey, top). The boundary between the plagioclase and orthopyroxene grains is open

Small sulphide grains enclosed in orthopyroxene (Figure A4 9), plagioclase and along grain boundaries (Figure A4 6) were observed. The sulphides have been identified as pyrite, pyrrhotite, pentlandite and chalcopyrite. These phases account for the parts per million amounts of copper and nickel in the rock.

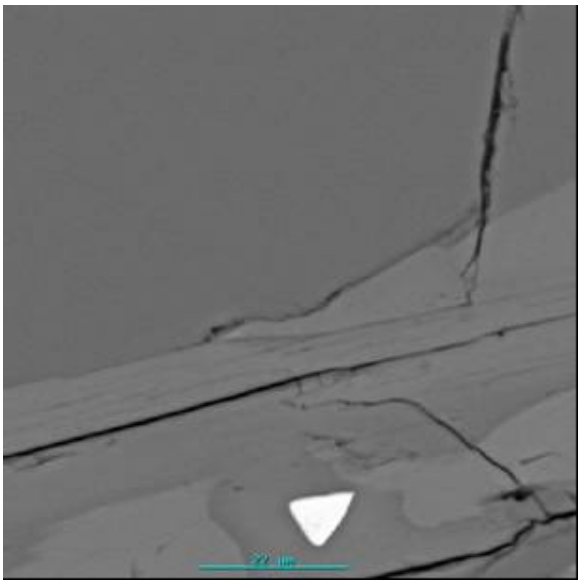

Figure A4 9 Triangular grain of sulphide enclosed in orthopyroxene (medium and light grey). The dark grey mineral at the top is plagioclase